The University of Melbourne

Master's Thesis

A Mathematical Model for Skip Segment Hirschsprung's Disease

Author:

Steven Maharaj

Supervisor:

Dr. James Osborne

Prof. Barry Hughes

A thesis submitted in fulfilment of the requirements

for the Master of Science

in the

School of Mathematics and Statistics

September 18, 2019

Declaration of Authorship

I, Steven Maharaj, declare that this thesis titled, "A Mathematical Model for Skip Segment Hirschsprung's Disease" and the work presented in it are my own. I confirm that:

- This work was done wholly or mainly while in candidature for a research degree at this University.
- Where any part of this thesis has previously been submitted for a degree or any other qualification at this University or any other institution, this has been clearly stated.
- Where I have consulted the published work of others, this is always clearly attributed.
- Where I have quoted from the work of others, the source is always given. With the exception of such quotations, this thesis is entirely my own work.
- I have acknowledged all main sources of help.
- Where the thesis is based on work done by myself jointly with others, I have made clear exactly what was done by others and what I have contributed myself.

Signed:

_____

Date:

_____

"Never give in, never give in, never, never, never, never-in nothing, great or small, large or petty - never give in except to convictions of honour and good sense. Never yield to force; never yield to the apparently overwhelming might of the enemy."

Winston Churchill

THE UNIVERSITY OF MELBOURNE

Abstract

Faculty of Science

School of Mathematics and Statistics

Master of Science

A Mathematical Model for Skip Segment Hirschsprung's Disease

by Steven Maharaj

Hirschsprung's disease (HD) is a condition that affects the normal peristaltic function of the gut. The condition is present at birth as a result of missing nerve cells in the muscles of the baby's colon. Skip segment Hirschsprung's disease (SSHD) is a special case of HD where a region of healthy gut is surrounded by unhealthy gut. Continuum models can successfully describe the behaviour of cell invasion and therefore infer probable reasons as to why and individual has HD. Unfortunately, very little is known about SSHD. In this thesis we develop a continuum model for SSHD and perform *in silico* experiments to better understand the nature of SSHD.

Acknowledgements

James and Barry, thank you for the amazing Msc experience. Thank you for being patient when I did not understand something. Thank you for always caring about my research. From the incompetent first year I was, both of you have shaped me into a very dangerous mathematician.

James, thank you for showing me numerical methods. Coming out of this project and your CDEs course has opened up a new world of possibilities for me. Now I see the world in triangles. Triangles that can now be solved.

Barry, thank you for showing me proper analysis. You showed me how to understand concepts at a very deep level and express them rigorously. Your unnatural attention to detail is amazing. I hope one day I can be on your level.

To my family, I love you all. I should tell you this more often. To my parents, thank you for supporting me throughout my education. As I get older I realise how much you had to sacrifice. To my brother Shaun, thank you for all our adventures.

À ma petite copine Clé, merci de ton bon coeur. Je suis vraiment désolé d'avoir passé autant de temps sur cette thèse. Je t'aime.

To the boys of G90 and G12, thank you for all the laughs. I will miss all of you after masters.

Contents

List of Figures

List of Tables

List of Abbreviations

ANS	**A**utonomic **N**ervous **S**ystem
CA	**C**ellular **A**utomata
CAM	**C**horio **A**llantoic **M**embrane
CNS	**C**entral **N**ervous **S**ystem
ENS	**E**nteric **N**ervous **S**ystem
GDNF	**G**lial cell line-**D**erived **N**eurotrophic **F**actor
HD	**H**irschsprung's **D**isease
MOL	**M**ethod **O**f **L**ines
NC	**N**eural **C**rest
ODE	**O**rdinary **D**ifferential **E**quation
PDE	**P**artial **D**ifferential **E**quation
PNS	**P**eripheral **N**ervous **S**ystem
SSHD	**S**kip **S**egment **H**irschsprung's **D**isease
TCA	**T**otal **C**olonic **A**ganglionosis

Chapter 1

Introduction

Hirschsprung's disease (HD) [1] is a congenital birth defect that affects the large intestine and causes problems with healthy bowel function. This disease occurs in 1 in 5000 newborns and if left untreated it can lead to death. The condition is present as a result of missing nerve cells in the muscles of the baby's colon. Signs and symptoms of Hirschsprung's disease vary with each case. Symptoms appear shortly after birth, but sometimes they're not apparent until later in life. Typically, the most obvious sign is a newborn's failure to have a bowel movement within 48 hours after birth. The only treatment for Hirschsprung's disease is surgery to bypass or remove the diseased part of the colon.

Skip segment Hirschsprung's disease (SSHD) [2] is a rare case of HD. In SSHD a 'skip area' consists of healthy gut segments surrounded proximally and distally by diseased gut segments. Although more than 30 cases have been reported in the literature [3], SSHD's existence remains controversial. This is due to the fact that there is no clear embryological theory to explain this phenomenon.

Fortunately, mathematical modelling and *in silico* experiments have provided us with a wealth of information about the invasion process. Among many other insights,

these models can infer things such as dominant invasion mechanisms, threshold parameters for HD, effects of chemical signalling and linage tracings of individual cells.

HD has been very well studied and there exist a large array of mathematical models of this phenomenon. Using a HD model as a foundation we construct a model for SSHD.

1.1 Thesis Overview

In order to understand the proposed model for SSHD, this thesis is structured so that the reader will be provided with the necessary biological and mathematical knowledge.

Chapter 2 outlines the necessary biological background for this work. Knowledge of these biological processes is paramount for modelling NC cell invasion accurately. The information presented in this chapter serves as the context in which we draw conclusions from our model.

In Chapter 3, we provide a literature review of previous modelling approaches describing the formation of the ENS. In particular, the history of continuum descriptions applied to HD is emphasised as this will be our model of choice for constructing the SSHD model.

In Chapter 4, the mathematical and computational framework of continuum models is presented. From a simple diffusion model, we build up to an advection-reaction-diffusion model which gives an accurate description of NC invasion.

In Chapter 5, we introduce a continuum model for SSHD. *In silico* investigations are performed to gain further insights into our new model.

The final chapter, Chapter 6, contains a discussion of the results and corresponding biological interpretations. We conclude with an outline of possible directions for future work.

Chapter 2

Biological Motivation

In order to construct an accurate model for SSHD or more generally any biological phenomenon one must first have knowledge about the system of interest from a non-mathematical perspective. In this chapter we will outline the biological structures on which we will base our mathematical model. First we provide a general discussion of the nervous system. Both HD and SSHD originate from a division of the nervous system called the enteric nervous system (ENS) so particular emphasis is given to this division. In the final section further details of HD and SSHD are outlined.

2.1 The Nervous System

In this section we detail the structural and physiological aspects of the nervous system. For the sake of clarity we have provided a visual depiction of the nervous system given by Figure 2.1. Each node in Figure 2.1 are detail in the subsections below.

2.1.1 A General Overview

The nervous system coordinates bodily functions via the transmission of electrical signals. In vertebrates it consists of two main parts, the central nervous system (CNS)

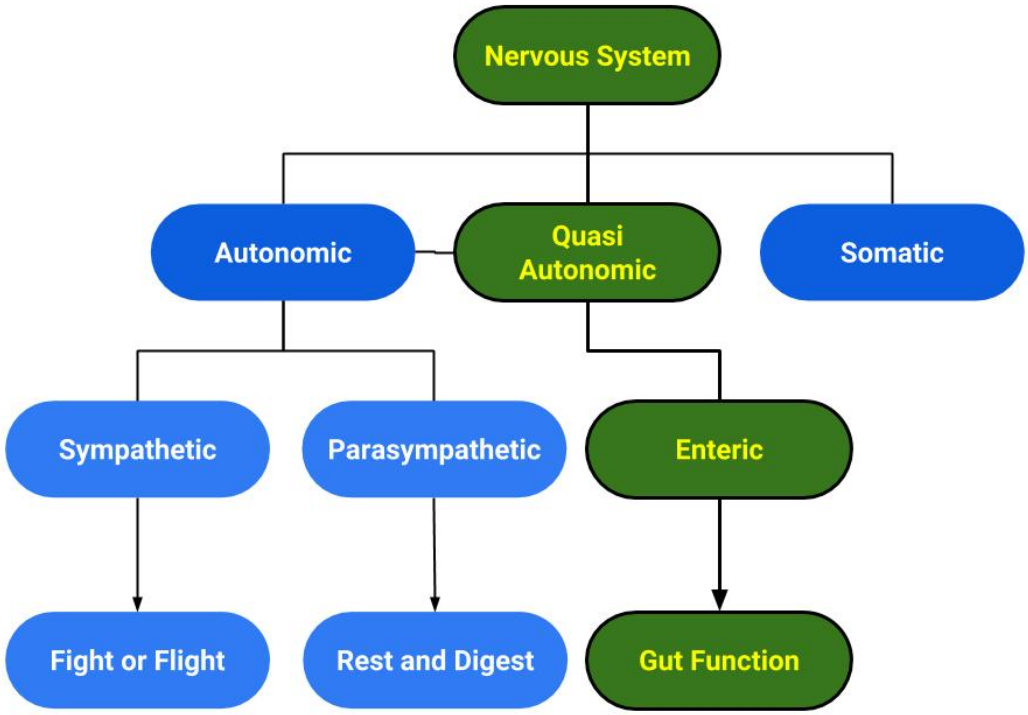

FIGURE 2.1: A visual representation of the nervous system. The path emphasised in green is where HD and SSHD occur.

and the peripheral nervous system (PNS). The CNS consists of the brain and spinal cord. The PNS consists mainly of nerves, which are enclosed bundles of the long fibres called axons, that connect the CNS to all other parts of the body. Nerves that transmit signals from the brain are called motor or efferent nerves, while those nerves that transmit information from the body to the CNS are called sensory or afferent nerves. The subsystem responsible for voluntary actions is termed the somatic nervous system while the subsystem responsible for involuntary actions is termed the autonomous nervous system (ANS). This thesis is not concerned with the somatic nervous system so further

details about this subsystem are omitted. The somatic nervous system has been well studied so any elementary text will enlighten a curious reader [4].

The ANS regulates many physiological processes. Some examples include: airway resistance, blood flow, blood pressure, body temperature, digestion, energy balance, excretion of wastes, fluid volume, glucose homoeostasis, heart rate, immune system, inflammatory processes, glandular secretions, papillary diameter, salt and water balance, and sexual function [5].

The ANS is divided in to three 'divisions': the sympathetic nervous system (SNS), the parasympathetic nervous system (PSN) and the enteric nervous system (ENS) . The SNS is sometimes referred to as the 'fight or flight' division as it plays a major role in response to danger, threats, and stress [5]. The PNS is often referred to as the 'rest and digest' division in recognition of its role in conserving energy, promoting digestion, and ridding the body of wastes [5]. The reader should note that the above summary of the ANS is extremely simplified as both divisions can work synergistically and therefore, does not fully encompass roles of each division. For more details on the ANS refer to Erica *et al.* [5].

2.1.2 Enteric Nervous System

The ENS is the third division of the nervous system. It resides in the wall of the gastrointestinal tract. It controls gut function and can still function even if separated from the CNS. However, the ENS is not classified as autonomous as it works in conjunction with the PNS and SNS and coordinates with the CNS to control digestive function so some authors use the term 'quasi autonomic' to describe the ENS [5, 6].

The ENS consists of small groups of nerve cells, enteric ganglia. The neural connections between these ganglia, and effector tissues, ensure healthy function of the muscles

of the gut wall, the epithelial lining, intrinsic blood vessels and endocrine cells [6].

Some other examples of the roles the ENS plays include: determining the patterns of movement of the gastrointestinal tract; controlling gastric acid secretion; regulating movement of fluid across the lining epithelium; changing local blood flow; modifying nutrient handling; and interacting with the immune and endocrine systems of the gut [6].

The formation of the enteric nervous system (ENS) arises from the migration of neural crest (NC) cells. Although NC cells are found along the entire length of the body, studies by Yntema and Hammond [7] showed that the ENS is derived from neural crest cells that originate from two specific regions; the vagal region (defined adjacent to somites 1-7) and the sacral region (caudal to somite 28 in chick embryos and caudal to somite 24 in embryonic mice and humans) Figure 2.2 shows the origins of neural crest cells that colonise the developing gastrointestinal tract [8].

The migratory behaviour of NC cells in the gut is also influenced by chemotaxis (movement associated with a chemical gradient). Glial cell line-derived neurotrophic factor (GDNF), which is expressed by the gut mesenchyme (a type of connective tissue), is chemoattractive to NC cells and appears to induce vagal cells to enter the gut and may also promote their rostro-caudal (mouth to anus) migration along the gut. The mathematical models in this thesis do not take into account the effects of chemotaxis. Many mathematical models have been developed to understand how chemotaxis influences the occurrence of Hirschsprung's Disease (formally introduced below) [9, 10, 11] but in the context of skip segment Hirschsprung's Disease (also formally introduced below) this would be a topic for further research.

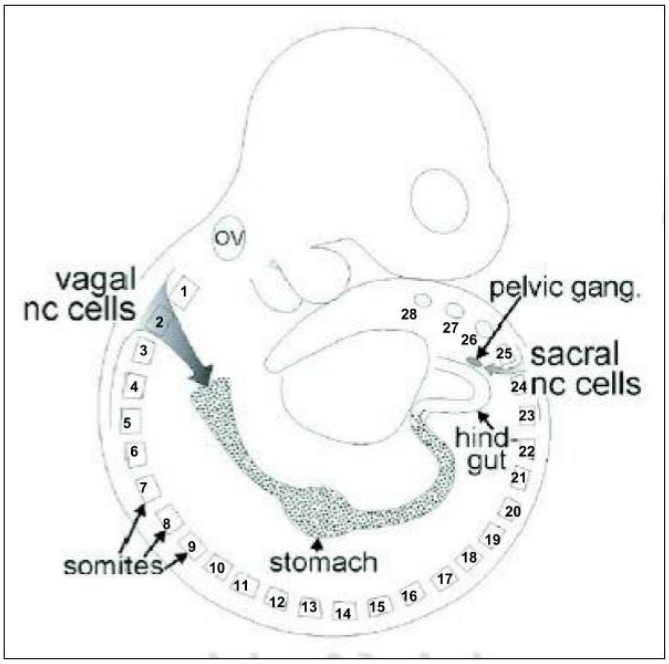

FIGURE 2.2: Modified from Anderson *et al.* [8]. Diagram of an embryo showing the origins of NC cells that colonise the developing gastrointestinal tract.

2.2 Development of the Gut

HD and SSHD are both congenital conditions, meaning that they are present from birth. Therefore, we will present an overview of gut development during the fourth to eighth weeks of embryogenesis in humans as this is primarily associated with the ENS formation.

During the fourth week of gut development, folding mechanisms give rise to the foregut, midgut and hindgut. By convention, the terms foregut, midgut, and hindgut

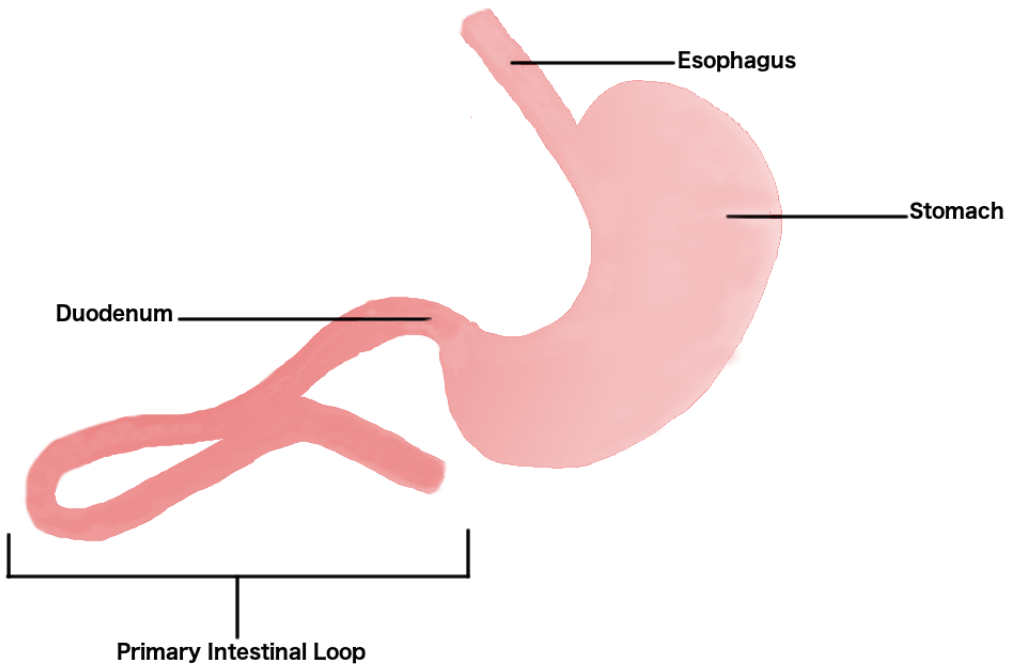

FIGURE 2.3: A diagram of the foregut and the midgut during the fifth week of development.

correspond to the territories of where the three major arteries feed into the developing gut [12].

In the fifth week, the foregut divides into the pharynx, esophagus, stomach, and proximal duodenum. Meanwhile in the midgut the distal duodenum, jejunum, ileum, cecum, ascending colon and proximal two thirds of the transverse colon begin to form. The future ileum elongates more rapidly than can be accommodated by the early peritoneal cavity (the space surrounding the abdominal walls) so that sometime during the fifth week the midgut folds and forms the 'primary intestinal loop'. Figure 2.3 gives an illustration of the primary intestinal loop. Lastly, the hindgut forms the distal third of

the transverse colon, the descending and sigmoid colon and the upper two thirds of the anorectal canal [12].

Between the sixth and eighth weeks, invading NC cells form the ENS.

2.3 Diseases of the Enteric Nervous System

2.3.1 Hirschsprung's Disease

Hirschsprung's disease (HD) is a congenital birth defect that affects 1 in 5000 newborns. The ganglia in the ENS fail to colonise the distal bowel but all other tissue is intact and functional. Under these circumstances, no propulsive activity (peristalsis) occurs in the aganglionic (without ganglia) bowel [6]. If the aganglionic bowel is not removed the individual will suffer from intestinal obstruction or severe constipation. This leads to an accumulation and dilation of the gut. Bacteria from the stool (fecal contents) can grow causing enterocolitis (inflammation of the digestive tract). Treatment for HD involves a pull-through surgery where the diseased segment of the large intestine is removed and the healthy segment is connected to the anus.

2.3.2 Skip Segment Hirschsprung's Disease

Skip Segment Hirschsprung's Disease (SSHD) is a rare phenomenon, involving a 'skip area' in a normally ganglionated intestine, which is surrounded proximally and distally by aganglionosis. Often SSHD is associated with total colonic aganglionosis (TCA) which was first reported by Zuelzer and Wilson [13], who suggested that aganglionosis could extend from the duodenum to the rectum. This is in contrast to HD as aganglionosis only occurs in the the distal bowel.

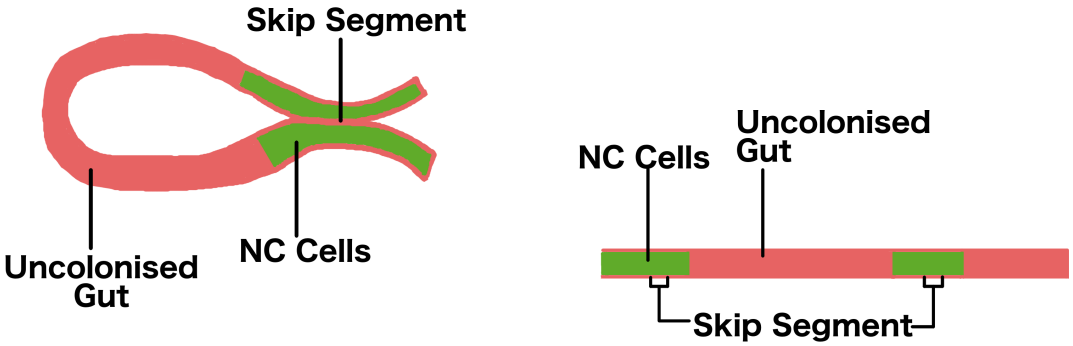

(A) (B)

FIGURE 2.4: 2.4a illustrates how rostral segments of the gut make contact with caudal sections of the gut which leads to SSHD. 2.4b idealises the gut as a one dimensional strip which will be used in Chapter 4 and Chapter 5 to build a mathematical model.

SSHD has no clear embryological explanation and its diagnosis may be missed as it is rarely suspected during surgery [3]. Biologists[1] hypothesise that the rare skipping phenomenon occurs when a rostral section of the gut is in contact with a caudal section of the gut due to the intestinal folding from the primary intestinal loop. Figure 2.4a shows this contact between the two ends of the gut. Figure 2.4b idealises Figure 2.4a as a one dimensional strip which we will later use in Chapter 4 and Chapter 5 to construct a mathematical model for invasion.

2.4 Summary

The nervous system coordinates actions by transmitting signals to and from different parts of the body. The division of the nervous system of interest to us is the ENS which

[1]The biologists collaborate with the School of Mathematics but are unnamed due to reasons of confidentiality.

regulates normal gut function.

During embryogenesis (in humans) the gut begins to form during the fourth to eighth weeks of development. Here NC cells invade the gut to form the ENS. This is what we will model in Chapter 4 and Chapter 5. When the NC cell population fails to colonise the gut the individual with present with HD. In rare cases there are sections of aganglionosis between normal ganglionated areas as in Figure 2.4. This condition is called SSHD.

Chapter 3

Literature Review

In this Chapter a literature review of relevant research on NC cell invasion is given. First we provide the reader with a review of the biology of NC invasion to form the ENS. In light of this background knowledge, we review possible mathematical models for this process. Continuum models and cellular automata (CA) models will both be discussed, but particular emphasis is placed on continuum models, as they will be used in later chapters to describe both HD and SSHD.

3.1 Biological Investigations

Evidence that NC cells could move was first published in 1869, only about 30 years after the theory of cells was proposed. Wilhelm His hypothesised that NC cells move away from a starting position to form nerve ganglia [14]. We now know that many complex mechanisms drive the systematic movement of cells during embryogenesis.

Embryonic studies of enteric ganglia date back to as early as the 1930s [15]. It was not until 1954 that the exact origin of enteric nerve cells had been settled. Yntema and Hammond [7] confirmed that enteric ganglia were derived from vagal NC cells. Twenty years, later Douarin and Teillet [16] precisely established a timetable for chick-quail

NC cell migration in grafting experiments. A few years later, Allen and Newgreen had successfully timetabled NC cell invasion in fowl embryos using chorio-allantoic membrane (CAM) grafts [17]. These cells migrate to form the dorsal neural tube, ventrally into foregut and the rostral midgut. Eventually, NC cells fill the more caudal regions via rostro-caudal invasion within the developing gut.

A second population of the sacral NC cells, caudal to the 28th pair of somites, was also shown to contribute cells to the hindgut. However, the precise role of the sacral NC in ENS formation remained controversial for many years. Evidence supporting a role for sacral NC in ENS formation came from studies by Pomeranz and Gershon [18]. Using a monoclonal antibody (NC-1) that binds to migrating NC cells they traced the development of sacral NC cells.

Meanwhile, Webster [19] showed that in mice subjects 'knocking out' (removing) the *Ret* gene produced intestinal aganglionosis and the mutation in the human homologue was a major cause of HD. Webster suggested that a delay in migration of NC cells could result in them failing to populate the caudal most gut. This idea caused a discrepancy between the results of Douarin and Teillet [16] and Allen and Neewgreen [17] on one hand and Pomeranz and Gershon [18] on the other.

Newgreen *et al.* [20] sort to rectify the discrepancy. From their studies they showed that more rostral segments of the gut commenced rapid growth earlier than more caudal segments. Their data was consistent with the idea that a delay in the arrival of vagal NC cells at any point in the intestine could jeopardise the ability of cells to fully populate the rest of the gut. This suggested that the interaction between the gut growth and the cell motility could be associated with HD.

Two years later, Young *et al.* [21], using immunohistochemical labelling of migrating NC cells, described the rostro-caudal progression of vagal NC cells along the gut. In

their studies, a caudo-rostral invasion that could be attributed to early migrating sacral NC cells was not observed. The conclusions from these investigations were either that sacral NC cells do not contribute to the ENS, or if they do colonise the hindgut, then sacral cells either fail to be detected or show delayed expression of all the markers that labelled migrating vagal NC cells. An alternative possibility is that in order to colonise the hindgut, sacral NC cells may require the presence of vagal NC cells within the hindgut. Therefore, if the gut was removed and cultured before the arrival of vagal NC cells, or if their arrival within the hindgut was prevented by severing the bowel, any sacral NC cells already present within the bowel could not develop due to the absence of vagal NC cells, or of factors, or signalling molecules, released by them or their progeny [22]. This was an important finding as it suggested that NC cells colonise the gut unidirectionally. In particular vagal NC cells colonise the gut rostro-caudally while sacral NC cells colonise caudo-rostrally.

Naturally one may ask, what drives such directional migration? Hearn *et al.* [23] proposed that this was due to 'population pressure' whereby cells behind the wavefront push the proceeding population forward to fill the wavefront. In their model, vagal NC cells would be forced to move away from their point of entry in the foregut, causing them to migrate towards the unpopulated caudal gut regions. However, it is unlikely that this could apply to sacral NC cells, since these cells enter the gut when it is already extensively colonised by vagal cells, therefore there are no longer unpopulated regions to move into [22].

The investigations performed by Natarajan *et al.* [24] also did not support the idea of population pressure. They showed that by injecting small amounts of *Ret* into aganglionic parts of the gut, NC cells were found to either migrate rostro-caudally along the gut or caudo-rostrally in the esophagus. Thus it was concluded that signalling

mechanisms play a vital role in directing NC cell migration.

Young *et al.* [25] later demonstrated that GDNF is a chemoattractant for enteric neural cells that promotes growth and directed migration of vagal NC along the gut. Young *et al.* postulated that GDNF levels could be higher in more caudal areas that could act as GDNF 'sinks'. NC cells could then be attracted towards these areas with higher levels of GDNF, in a gradient dependent fashion.

3.2 Mathematical Models for NC Cell Invasion

In this section we will describe cell invasion on two levels: the local behaviour of individuals cells and the global properties of the group as a whole. Local behaviour of individuals cells is governed by a stochastic agent-based model, while the global properties of the group as a whole are governed by a partial differential equation (PDE) which describes the cell density as a continuous function.

3.2.1 Continuum Models

A continuum model gives us information about the macroscopic or global behaviour of a system. When microscopic movements result in some macroscopic or gross regular motion of the group of cells (or other particles) we can think of it as a diffusion process [26]. A diffusion process describing cell migration is an essential feature of many important biological systems, including wound healing, tumour invasion, and several developmental processes [26].

3.2.2 Fisher's Equation

However cell motility alone does not provide an accurate description of cell invasion in the gut. Typically, a system of conservation equations is proposed which incorporates the migratory processes in conjunction with kinetic terms to simulate proliferation of the migratory population. The Fisher-Kolmogorov (Fisher's) Equation [27] is the archetypal model that incorporates cell migration together with cell proliferation via a logistic process. Explicitly stated,

$$\frac{\partial u}{\partial t} = \underbrace{D\frac{\partial^2 u}{\partial x^2}}_{\text{Motility}} + \underbrace{ku\left(1-\frac{u}{C}\right)}_{\text{Proliferation}}.$$

We consider this to be a logistic process because in the long run of course there must be some bound on the cell proliferation. Verhulst [28] proposed that a self-limiting process should operate when the population becomes too large. The $ku(1-u/C)$ term in Fisher's Equation represents cell proliferation to some carrying capacity C.

Exact solutions of Fisher's Equation have been found [26, 29, 30, 31] but for only very special cases of the initial conditions. However, these special cases do not represent the biological observations from the formation of the ENS. Fortunately, wavespeeds of Fisher's Equation have been well studied. Therefore, when we solve Fisher's Equation in Chapter 4 we employ numerical techniques, then compare the numerical wavespeed with the theoretical wavespeed [26].

During the 2000s, many authors preferred to use this model to describe NC cell colonisation to form the ENS as a rostro-caudal wave. In 2006, Simpson *et al.* published two very important papers [11, 32] that mathematically confirmed the results from the biological investigation mention in the previous section [17, 20, 33]. Their studies [32] investigated the coupling of a set of cell host and donor populations, formally known as a

chimera experiment (some authors use the term 'kebab cultures' for chimera experiment [11, 32]). Their work suggested that NC cells on the wavefront act as the critical mechanism driving the directed invasion. Cells behind the wavefront are essentially non-proliferative and do not directly participate in the invasion of unoccupied tissues. This is known as the 'frontal expansion' process. This type of cell invasion further supports the idea that there is no population pressure from cells behind the wave front pushing those cells on the wave front forward.

Another conclusion from Simpson *et al.* [11] made was that 'logistic proliferation exerts the dominant control on the system'. This means proliferation is the critical mechanism driving invasion. Five migration mechanisms were considered: linear diffusion, two cases of nonlinear diffusion, chemokinesis and chemotaxis. The model results told us that the precise nature of the flux mechanism plays a minor role in comparison to the proliferation term. Further perturbation analysis revealed that the logistic proliferation term controls the shape of the invasion waves. This implied that it was the proliferation terms in the conservation equations that dominate and drive NC cell invasion models.

3.2.3 Growing Domains

NC invasion occurs during embryogenesis, meaning that while invasion takes place the gut is growing simultaneously. Therefore, gut growth must be incorporated into the mathematical model of NC cell invasion. This introduces a velocity field associated with the gut growth. The velocity field modifies the NC cell motility within the growing tissues.

Reaction-diffusion equations on growing domains have been well studied [34] and have been successfully applied to phenomena such as limb bud development [35] and

animal coat markings [36, 37, 38]. In this thesis we use the Growing Fisher's Equation,

$$\frac{\partial u}{\partial t} = \underbrace{D\frac{\partial^2 u}{\partial x^2}}_{\text{Motility}} + \underbrace{ku\left(1-\frac{u}{C}\right)}_{\text{Proliferation}} - \underbrace{\frac{\partial (vu)}{\partial x}}_{\text{Gut Growth}},$$

to model NC cell invasion in a growing gut. Note that v is the velocity field associated with the gut growth. Landman *et al.* [9] first considered a velocity that grew uniformly in space. They considered linear, exponential and logistic uniform domain growth models. Their models provided an insight into cell invasion during embryonic growth, and its dependence on the form and timing of the domain growth [9].

Two years later Simpson *et al.* [10] considered non-uniformly growing velocity fields. In their paper they developed a numerical a algorithm to solve the Growing Fisher's Equation on non-uniformly growing domains. This provided a more accurate description of cell migratory behaviours since it is well known in the biological literature that rostral areas of the gut grow more rapidly than caudal areas of the gut [20].

3.3 Cellular Automata Models

An alternative way to model NC cell invasion is to use a stochastic agent-based model also known as a cellular automata (CA) model. There are two types of agent-based models: lattice-based models, where agents move between sites of a lattice; and off-lattice models, where agents move freely without a lattice structure. Most biological or physical processes being modelled do not have an intrinsic lattice structure, making off-lattice models more realistic. However lattice based models often have the advantages of simpler calculations [39].

In the simpler lattice-based models a cellular agent at position (x, y) attempts to move to one of the four nearest neighbours $(x\pm1, y\pm1)$ each with equal probability. The cellular agent also attempts to divide into two daughter cells that are either deposited into $(x \pm 1, y)$ or $(x, y \pm 1)$ each with equal probability. If the target site is occupied then for any motility or proliferation event then that event is aborted. This is called the exclusion process [39, 40, 41]. This process is illustrated by Figure 3.1.

An advantage of the CA model is that one can track an individual cell though time. This is known as lineage tracing [42]. A single cell is marked and this mark is inherited by all progeny. The contribution of an individual cell lineage can then be traced within a population of cells. A pictorial representation of lineage tracing in shown in Figure 3.2.

An important concept discussed by Cheeseman *et al.* was that a few cells in the initial population were responsible for a great majority of the final cell population: these cells are called 'superstars' [41]. Cheeseman *et al.* explored the two main cases of the invasion process, the non-growing domain and the growing domain. For a non-growing domain superstars produced a 'disproportionately huge number of progeny,' while for the case of the growing domain superstars produced a less significant number of progeny.

3.4 The Relationship between Continuum Models and Cellular Automata Models

There exists an intimate relationship between continuum models and CA models. In fact it can be shown that by taking appropriate continuum limits we can derive one model from the other. First one would start with the CA model then take average

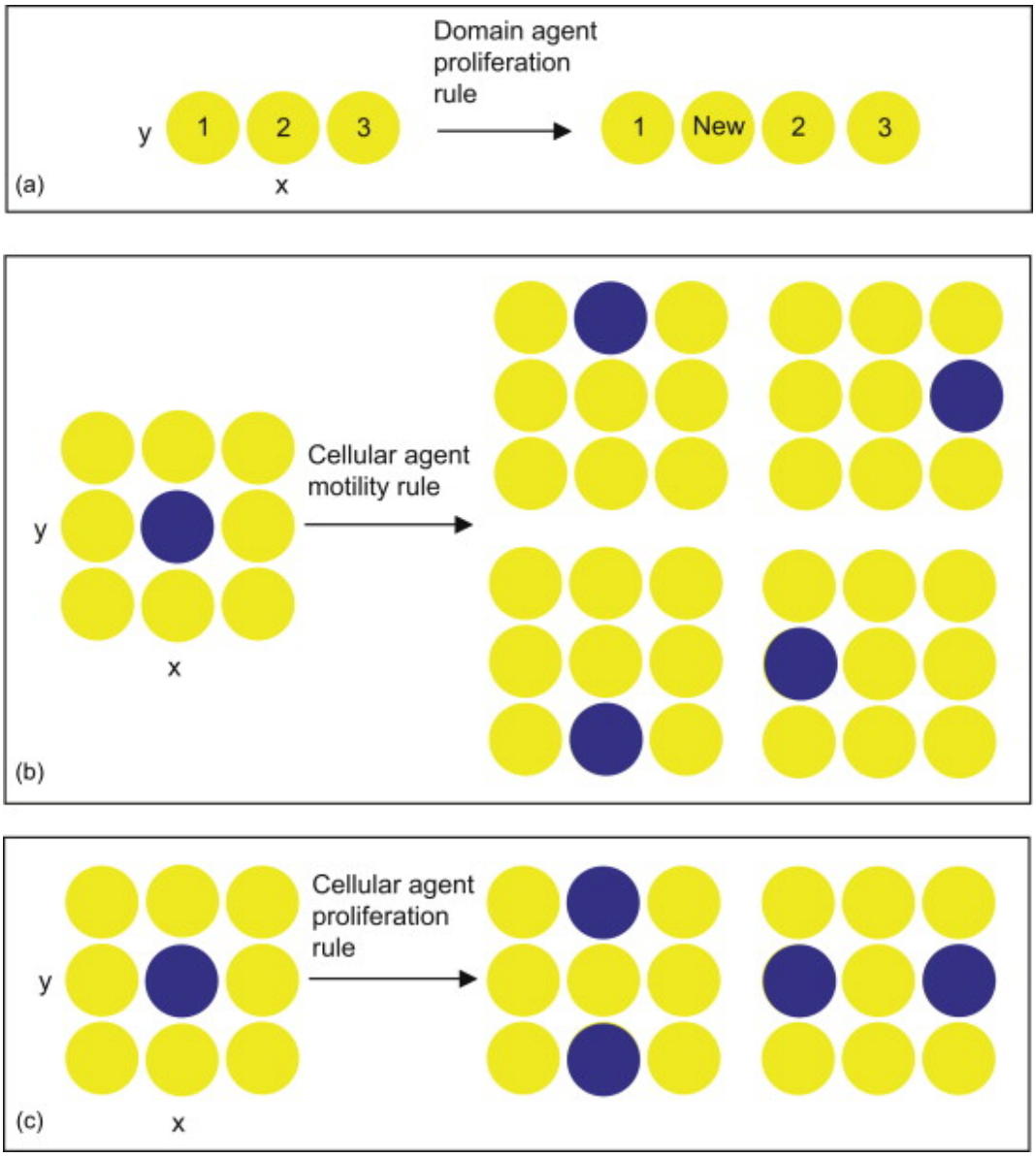

FIGURE 3.1: Modified from Binder and Landman [40]. (a) illustrates the proliferation rule for a single domain agent (yellow). (b) illustrates the motility rules for a single cellular agent (blue). The cellular agent can move to one of the four configurations shown with equal probability. (c) illustrates the proliferation rules for a single cellular agent. The mother cellular agent divides into two daughter agents. After mitotic division two possible configurations can occur with equal probability.

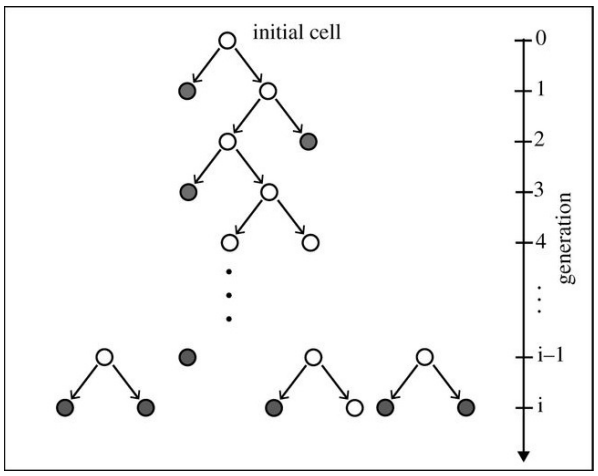

FIGURE 3.2: Modified from Cheeseman *et al.* [41]. Lineage of a single agent at generation i. An empty circle represents an agent division event. Only the grey-filled circles are counted to determine the agent lineage.

densities of the cellular agents. This yields a Fokker–Planck type of PDE with an addition advective term to account for gut growth [40].

This averaging approach was verified by Binder *et al.* [43] on a specific case study involving the developing intestinal tract of quail embryos. The averaging of the discrete results predicted population-level properties of the system which match those of the continuous model [43].

Penington *et al.* [39] very elegantly extended the CA model by allowing agents to be an arbitrary length and move an arbitrary distance per time step although there was no proliferation in their model. When average densities were taken a diffusion equation with a non-linear diffusion coefficient term was obtained as opposed to the regular CA model where if we take an average of the discrete agents it yields a diffusion equation with a linear diffusion coefficient term.

3.5 Summary

In this section we provided the reader with a review of the biology of NC invasion to form the ENS. Given this background knowledge, we then provided a review of possible mathematical models for this process. There were two ways to model cell invasion: continuum models using PDEs or cellular automata models using stochastic based arguments. Below in Figure 3.3 is a timeline summary of the essential biological and mathematical findings discussed in this chapter. We focused most of our attention on continuum models as this will be the model of choice for the next two chapters.

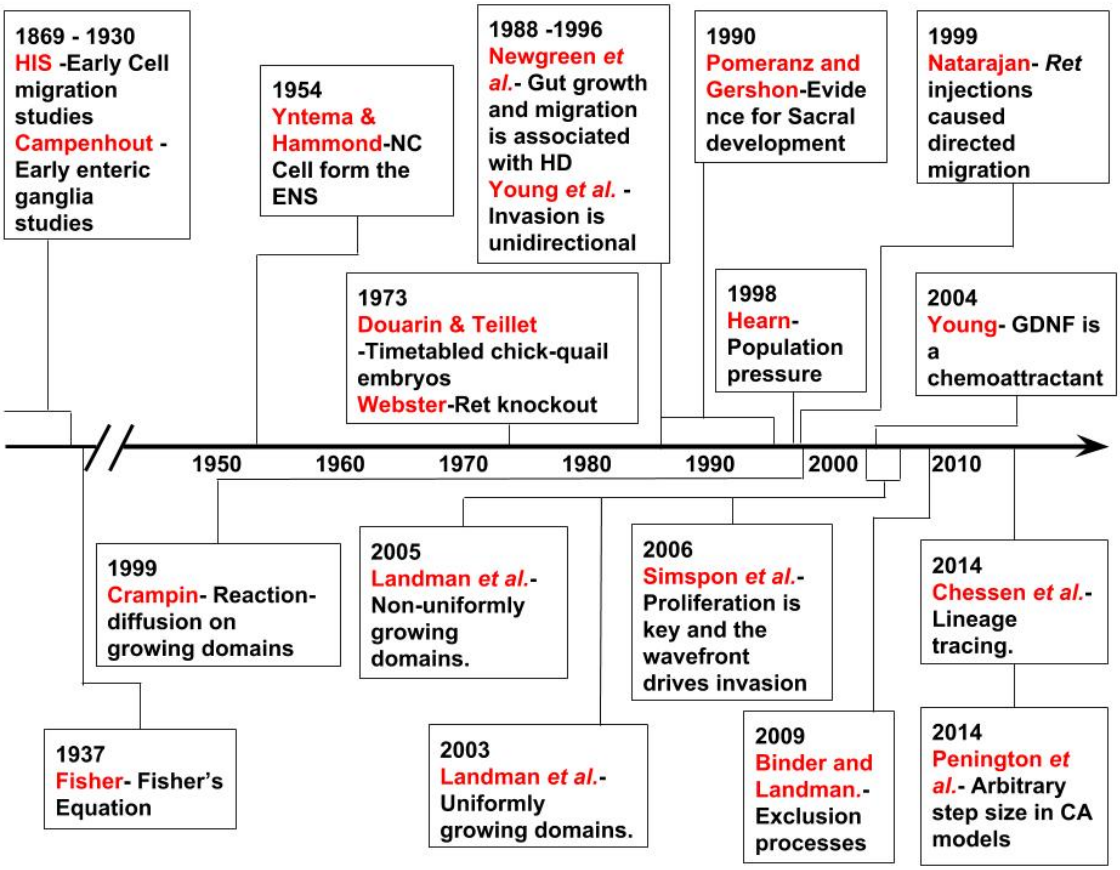

FIGURE 3.3: A timeline summary of the essential biological and mathematical findings discussed in this chapter. The upper level summarises biological findings while the lower level summarises mathematical findings.

Chapter 4

Mathematical and Computational Preliminaries

In this Chapter we build up the necessary mathematical preliminaries to model NC invasion to form the ENS. Each model we propose is based on the conservation of mass equation,

$$\frac{\partial u}{\partial t} + \frac{\partial J}{\partial x} = S, \tag{4.1}$$

where J is the flux and S is the source term. First, we discuss diffusion (representing cell motility) then reaction-diffusion (representing motility and cell proliferation) and finally a advection-reaction-diffusion equation (representing motility and cell proliferation in a growing gut).

All continuum models are solved using the method of lines (MOL). In this approach the PDE is first discretised in space. This gives a large system of ODEs with each component of the system corresponding to the solution at some grid point, as a function of time. The system of ordinary differential equations (ODEs) can then be solved using numerical ODE techniques [44]. This method is also often called a semi-discrete method, since we have discretized in space but not in time [44]. For the ODE systems in this

thesis we will take advantage of MATLAB's in-built ODE solvers [45].

4.1 Diffusion

In this section we will solve the diffusion equation analytically and numerically. The MOL algorithm will be discussed in detail so all results in this thesis can be reproduced. Lastly, the numerical solution will be compared with the exact solution as a check of accuracy.

4.1.1 Mathematical Model

Consider the diffusion (heat) equation,

$$\frac{\partial u}{\partial t} = D\frac{\partial^2 u(x,t)}{\partial x^2}, \tag{4.2}$$

where $u = u(x,t)$ is the the cell density; $x \in [0, X]$ represents the longitudinal position in the gut; time $t \geq 0$ and D is the diffusion coefficient. For this model,

$$J = -D\frac{\partial u}{\partial x}, \quad S = 0.$$

Note that by taking D to be a constant we have linear diffusion. Examples of non-linear diffusion have be studied by Simpson *et al.* [11, 32].

We apply the following scaling,

$$x = \sqrt{D}x^*.$$

Dropping the asterisk notation we have

$$\frac{\partial u}{\partial t} = \frac{\partial^2 u}{\partial x^2}, \quad \text{for} \quad x \in \left[0, X/\sqrt{D}\right], \quad t \geq 0. \tag{4.3}$$

For simplicity we set $X/\sqrt{D} = 1$.

We impose no flux (zero Neumann) boundary conditions,

$$\left.\frac{\partial u}{\partial x}\right|_{x=0} = 0, \qquad \left.\frac{\partial u}{\partial x}\right|_{x=1} = 0. \tag{4.4}$$

Although, Dirichlet boundary conditions are simpler to implement numerically, Neumann boundary conditions are preferred because in the next section we reproduce results from Simpson *et al.* [11, 32] which involves solving a reaction-diffusion equation with no flux boundary conditions.

For the initial condition we choose,

$$u(x, 0) = \cos(\pi x).$$

Therefore, an analytic solution of Equation (4.3) can easily be determined using separation of variables.

In Appendix A we show,

$$u(x, t) = \cos(\pi x) e^{-\pi^2 t}.$$

4.1.2 Computational Model

Next we will construct a computational model from the MOL. A full elementary treatment of this method is provided.

First, divide the spacial domain into $N+1$ mesh points or N sub-intervals each with length $h = 1/N$. Using a central finite difference approximation the second derivative term can be approximated:

$$\frac{\partial^2 u_i}{\partial x^2} \approx \frac{u_{i-1} - 2u_i - u_{i+1}}{h^2}, \tag{4.5}$$

where $u_i = u(x_i, t)$ and x_i for $i = 1, 2, \ldots, N+1$ is a mesh point. Note that the central finite difference approximation is a second order method which is more accurate than a first order method such as forward difference or backward difference [44]. The left hand side of Equation (4.3) does not contain any derivatives in x so it can be simply approximated as

$$\frac{\partial u}{\partial t} \approx \frac{du_i}{dt} = \dot{u}_i.$$

Thus, the full computational model is

$$\dot{u}_i = \frac{u_{i-1} - 2u_i - u_{i+1}}{h^2}.$$

Next, the no flux boundary conditions are incorporated into the model. A technique called ghost noding [44] is employed. This involves creating two fictitious mesh points at the ends of the spacial domain (say u_0 and u_{N+2}). Under this assumption one can show that

$$u_0 = u_2, \quad u_N = u_{N+2}.$$

This yields the full system,

$$
\begin{aligned}
\dot{u_1} &= \frac{2u_2 - 2u_1}{h^2}, \\
\dot{u_2} &= \frac{u_3 - 2u_2 + u_1}{h^2}, \\
&\vdots \\
\dot{u_{N-1}} &= \frac{u_N - 2u_{N-1} + u_{N-2}}{h^2}, \\
\dot{u_N} &= \frac{2u_{N-1} - 2u_N}{h^2}.
\end{aligned}
$$

It is usually more computationally efficient to code such systems as matrices. In matrix form our system is

$$
\begin{bmatrix} \dot{u_1} \\ \vdots \\ \\ \\ \\ \\ \\ \vdots \\ \dot{u_{N+1}} \end{bmatrix} = \frac{1}{h^2} \begin{bmatrix} -2 & 2 & & & & & & & \\ 1 & -2 & 1 & & & & & & \\ & \ddots & \ddots & \ddots & & & & & \\ & & & & & & & & \\ & & & & \ddots & \ddots & \ddots & & \\ & & & & & 1 & -2 & 1 & \\ & & & & & & 2 & -2 & \end{bmatrix} \begin{bmatrix} u_1 \\ \vdots \\ \\ \\ \\ \\ \\ \vdots \\ u_{N+1} \end{bmatrix}.
$$

4.1.3 Cross Validation

Since there is a closed form solution to Equation (4.3) we can validate our numerical solution. Figure 4.1a shows the time evolution of the exact solutions overlaid with the numerical solution. The MOL algorithm seems to have approximated the solution accurately. Also, it should be noted that no mass has entered or exited the system.

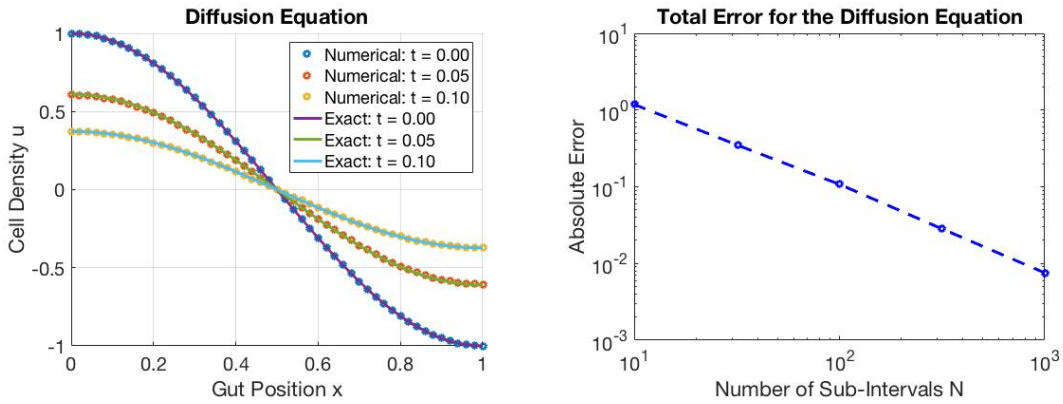

(A) Diffusion profile (B) Error plot

FIGURE 4.1: (4.1a) compares the numerical solution plotted with the exact solution over time of the diffusion model. (4.1b) is a log-log plot of the total absolute error for various N.

Therefore since the initial condition integrates to zero the steady state solution is also zero.

Figure 4.1b shows the total absolute error decreasing as N (the number of sub-intervals) increases. Using a central finite difference approximation will force the spacial error to be second order. This is verified in Figure 4.1b as the gradient of the error plot is observed to be -2.

Finding the error in time is more ambiguous as the temporal variable is not discretised. The diffusion equation is numerically a 'stiff problem' [44] so a stiff ODE solver was used to find the solution. The MATLAB solver `ode15s` [45] was use to solve our problem. This solver uses a backward differentiation formula of varying order.

4.2 Fisher's Equation

The next model we consider is a type of reaction-diffusion equation called the Fisher's Equation sometime called the Kolmogorov–Fisher Equation. This is a nonlinear differential equation so the analytic solution only exists for special choices of the initial condition [26, 29, 30, 31]. Instead we choose to compare the theoretically produced wave speed with our numerically outlined wave speed.

4.2.1 Mathematical Model

For this model we set,

$$J = -D\frac{\partial^2 u}{\partial x^2}, \quad S = k\left(1 - \frac{u}{C}\right)$$

and so Fisher's Equation is,

$$\frac{\partial u}{\partial t} = D\frac{\partial^2 u}{\partial x^2} + ku\left(1 - \frac{u}{C}\right), \quad \text{for} \quad x \in [0, X], \quad t \geq 0, \tag{4.6}$$

where D is the diffusion coefficient, k is the mitotic index and C is the carrying capacity. Again, we impose no flux boundary conditions given by Equation (4.4).

Applying the following scaling,

$$u = Cu^*, \quad x = \sqrt{\frac{D}{k}}x^*, \quad t = \frac{1}{k}t^*,$$

dropping the asterisk notation we have

$$\frac{\partial u}{\partial t} = \frac{\partial^2 u}{\partial x^2} + u(1-u), \quad \text{for} \quad x \in \left[0, X\sqrt{\frac{k}{D}}\right], \quad t \geq 0. \tag{4.7}$$

In order to see travelling wave behaviour the right boundary is set to a value large enough to avoid boundary effects on the right. We choose,

$$X\sqrt{\frac{k}{D}} = 300,$$

similar to Simpson *et al.* [11, 32].

The initial condition is chosen to be in the form of a Heaviside function,

$$u(x, 0) = \mathrm{H}(100 - x).$$

Due to the non-linearity in Fisher's Equation there is not always an analytic solution. Instead we will follow Murray [26] and use linear stability analysis to better understand this model [26].

For Equation (4.7) we try the travelling wave solution of the form,

$$u(\xi, \tau) = U(z), \quad z = \xi - c\tau, \tag{4.8}$$

where c is the wave-speed. Since Equation (4.7) is invariant under the replacement of x by $-x$ without loss of generality we assume $c \geq 0$. This yields the first order ODE,

$$U'' + cU' + U(1 - U) = 0. \tag{4.9}$$

Next, we let $V = U'$. This gives the system

$$\begin{aligned} U' &= V, \\ V' &= -cV - U(1 - U). \end{aligned}$$

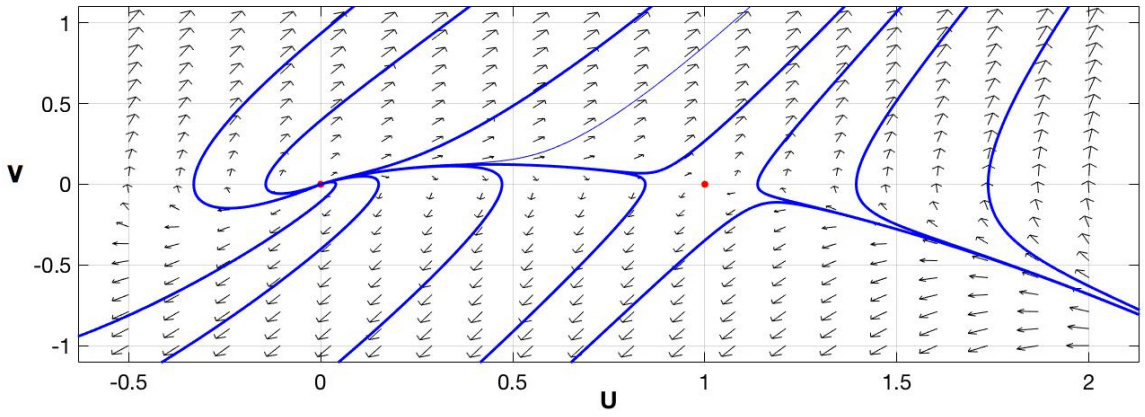

FIGURE 4.2: A phase plane diagram of (U, V) when $c = 2$. The points (0,0) and (1,0) are fixed points of the system (red dots). At (0,0) there is stable node while at $(1, 0)$ we have a unstable saddle point.

Performing linear stability analysis on U and V, one can show that the fixed points are

- $(U, V) = (0, 0)$ with eigenvalues

$$\lambda_1 = \frac{-c + \sqrt{c^2 - 4}}{2} \quad \text{and} \quad \lambda_2 = \frac{-c - \sqrt{c^2 - 4}}{2},$$

- $(U, V) = (1, 0)$ with eigenvalues

$$\lambda_3 = \frac{-c + \sqrt{c^2 + 4}}{2} \quad \text{and} \quad \lambda_4 = \frac{-c - \sqrt{c^2 + 4}}{2}.$$

For the fixed point at $(0, 0)$, if $0 < c < 2$ we have a stable spiral. In this case the trajectories are physically unrealistic as U could take negative values. In the case $c \geq 2$ we have a stable node. For the fixed point at $(1, 0)$ we have a saddle point which is always unstable. Figure 4.2 shows the phase plane trajectories for $c = 2$. In their initial paper, Kolmogorov et al. [46] showed that all initial conditions with compact support

evolve to the travelling wave with the minimum speed of 2, which is the case for our problem. Note that for the dimensional system one has $c = 2\sqrt{kD}$.

4.2.2 Computational Model

Constructing a computational model is done by applying the central finite difference approximation to Equation (4.7). This yields

$$\frac{\partial u_i}{\partial t} = \frac{u_{i-1} - 2u_i - u_{i+1}}{h^2} + u_i(1 - u_i). \tag{4.10}$$

Figure (4.3) shows the travelling wave solutions of Equation (4.7). The density grows to a carrying capacity of $u = 1$ due to the logistic reaction term, while the diffusion term causes a wavelike dispersal outward.

4.2.3 Cross Validation

Now that we have derived the wave speed we are able to validate the numerical solution for Equation (4.7). As shown above one would expect the numerical wave speed to be 2. This is the case once the growth term begins to dominate the diffusive term in Equation (4.7). Characteristic curves allow us to clearly visualise the wavefront evolving in time so one can track the wave speed. Figure (4.4a) compares the characteristics of a standard travelling wave with characteristics of the numerical solution. Figure(4.4b) shows the gradients of the characteristic curve (local wave speed) from Figure 4.4a. We find that as $t \to \infty$ the numerical wave speed approaches the theoretical wave speed, $c = 2$.

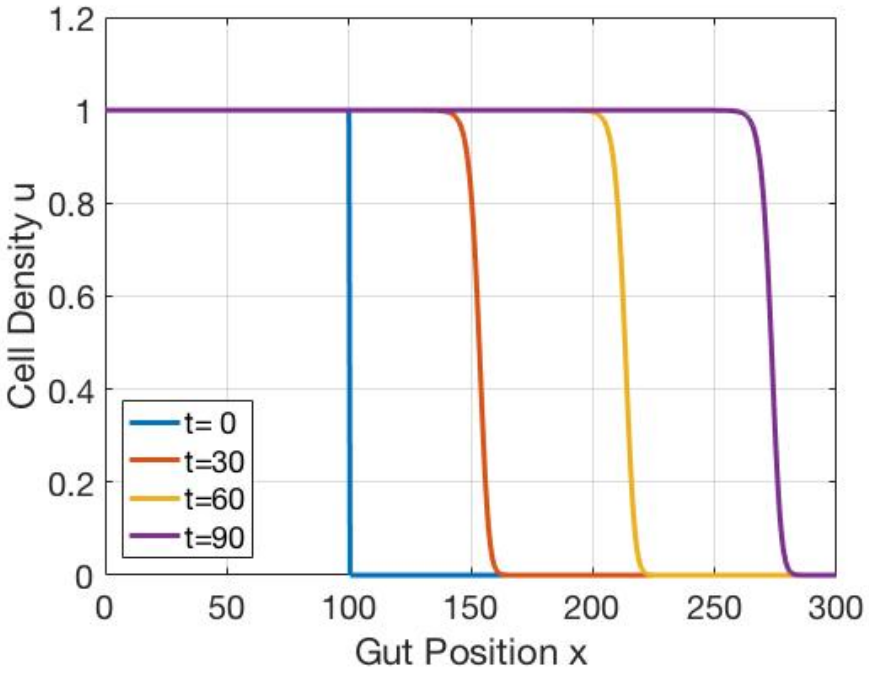

FIGURE 4.3: Travelling wave solution of Fisher's Equation from $t = 0$ to $t = 90$.

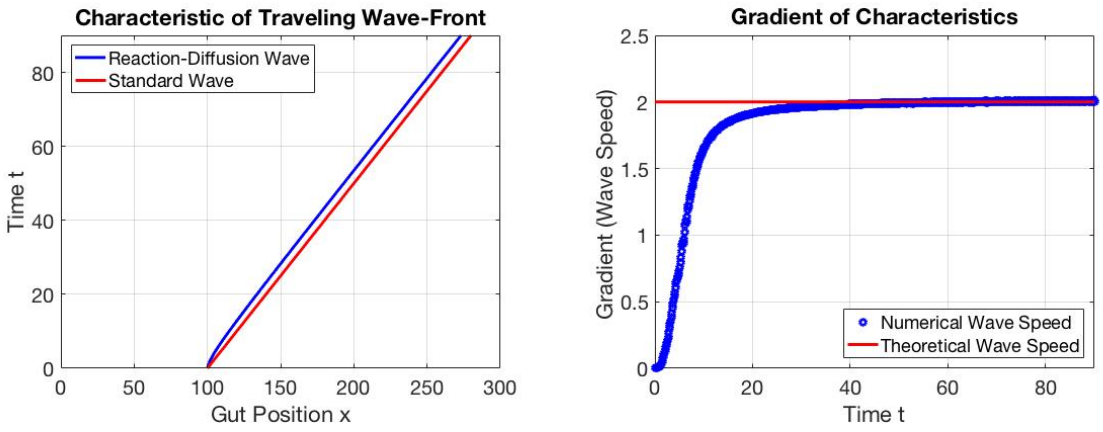

(A) Characteristic curves (B) Wave speeds

FIGURE 4.4: (4.4a) compares the characteristics of Fisher's Equation and a standard travelling wave with wave speed $c = 2$. Figure (4.4b) compares the gradients of characteristics through time. We can see that for large enough t the numerical wave speed attains the theoretical wave speed.

4.3 Growing Domains

Next we will investigate Fisher's Equation on a uniformly growing domain (Growing Fisher's Equation). The following model will be based on Landman *et al.* [9]. This thesis will only discuss uniformly growing domains. Non-uniform domain growth terms introduce hyperbolic terms which are slightly more difficult to implement numerically. Simpson *et al.* [10] give a full treatment of dealing with these hyperbolic terms in the context of ENS invasion.

4.3.1 Mathematical Model

The growth of the domain is described by a local velocity $v(x,t)$ such that a point x moves to the point $x + v(x,t)\Delta t$. By considering a small element Δx of the domain, it

can be shown that

$$\frac{dL}{dt} = \int_0^L \frac{\partial v}{\partial x} dx, \tag{4.11}$$

where $L = L(t)$ is the length of the domain at time t. A proof of this result is provided in Appendix B.

Under the uniform growth assumption $\partial v/\partial x$ is independent of x and is only a function of t, written as

$$\frac{\partial v}{\partial x} = \sigma(t).$$

Inserting this into Equation (4.11) we find that the velocity is given by

$$v(x,t) = \frac{1}{L}\frac{dL}{dt}x.$$

For this model $S = k(1 - u/C)$ but due to the domain growth the velocity contributes an additional advection term to the flux [26] so,

$$J = -\left(\frac{\partial u}{\partial x} - vu\right).$$

Thus the conservation equation can be written as

$$\frac{\partial u}{\partial t} = D\frac{\partial^2 u}{\partial x^2} + ku\left(1 - \frac{u}{C}\right) - \frac{\partial (v(x,t)u)}{\partial x}. \tag{4.12}$$

We introduce the dimensionless variables,

$$u^* = \frac{u}{C}, \quad x^* = \frac{x}{L_0}, \quad t^* = kt, \quad v^* = \frac{v}{kL_0},$$

where $L(0) = L_0$ and we have the dimensionless parameters

$$D^* = \frac{D}{kL_0^2}, \quad L^* = \frac{L}{L_0}.$$

This leads to Equation (4.12) becoming

$$\frac{\partial u}{\partial t} = D\frac{\partial^2 u}{\partial x^2} + u\,(1-u) - \frac{\partial (vu)}{\partial x}, \tag{4.13}$$

where the asterisk notation has been dropped. In order to solve Equation (4.13) one can fix the domain on $(0, 1)$ by introducing another scale $\xi = x/L$ [9, 34]. This transformation eliminates the advection term giving,

$$\frac{\partial u}{\partial t} = \frac{D}{L^2}\frac{\partial^2 u}{\partial \xi^2} + u\,(1-u) - u\frac{1}{L}\frac{dL}{dt}. \tag{4.14}$$

This is shown explicitly in Appendix C.

4.3.2 Computational Model

Applying the MOL to Equation (4.14) one can show that the correct spacial discretisation is

$$\frac{\partial u_i}{\partial t} = \frac{D}{L^2}\frac{u_{i-1} - 2u_i - u_{i+1}}{h^2} + u_i(1-u_i) + u_i\frac{1}{L}\frac{dL}{dt}. \tag{4.15}$$

Before this model can be solved one must decide how the domain grows by choosing some $L(t)$. Landman *et al.* [9] have investigated linear, exponential and logistic growth models. We will outline each model of growth and discuss their respective properties from the numerical solutions shown by Figure 4.5. Note that all Growing Fisher models are solved in the (ξ, t) variables and then transformed back to (x, t) to obtain the wave profiles and characteristic plots.

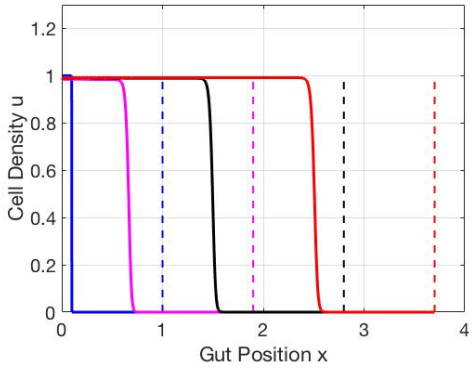

(A) Invasion Profile

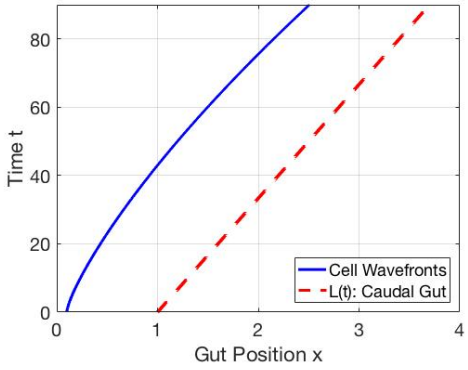

(B) Characteristics

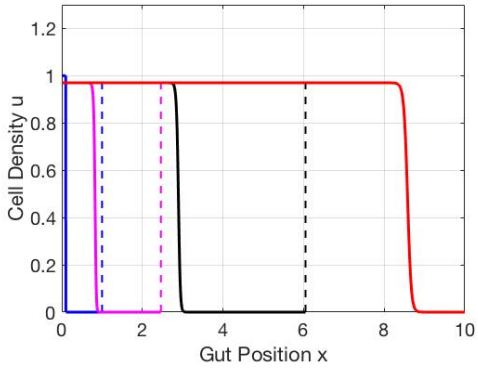

(C) Invasion Profile

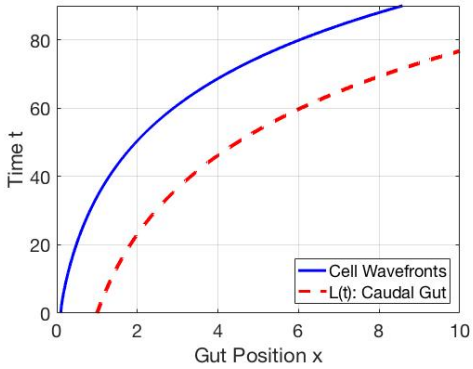

(D) Characteristics

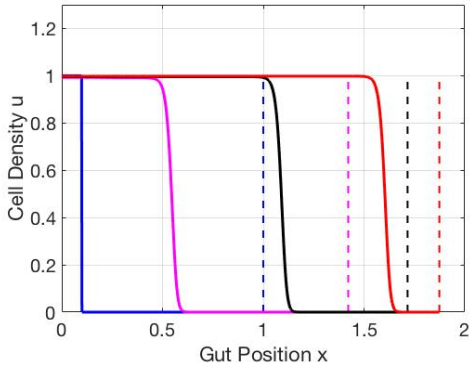

(E) Invasion Profile

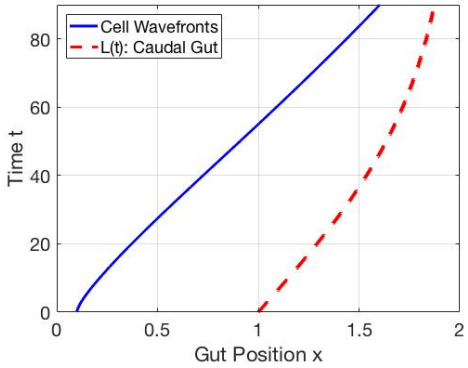

(F) Characteristics

FIGURE 4.5: Solutions of the Growing Fisher's Equation for linear (A and B), exponential (C and D) and logistic (E and F) gut growth. The left column displays the invasion profiles for $t = 0, 20, 40, 60$ (blue, magenta, black, red respectively) and the right column displays the corresponding characteristics. $D = 0.00004$ and $\alpha = 0.03$.

For linear growth,

$$L = 1 + \alpha t.$$

In Figure 4.5a D and α were chosen such that the wavefront of the travelling wave cannot overcome the domain growth. The cell wave front moves away from $L(t)$ and appears to track a straight line in the (x, t) plane.

In the case of exponential growth,

$$L = e^{\alpha t}.$$

We observe the same qualitative behaviour as linear growth. The only difference is that the cell wavefront tracks a curved line, rather than a straight line, in the (x, t) plane.

For logistic domain growth,

$$L = \frac{L_\infty}{1 + (L_\infty - 1)e^{-\alpha t}}.$$

In this model the domain has its own carrying capacity L_∞. Logistic growth differs from linear and exponential growth in that the domain length approaches L_∞. Hence the cell wavefront will always reach $L(t)$ in some finite time in Figures 4.5e and 4.5f we have set $L_\infty = 2$.

4.4 Modelling Hirschsprung's Disease.

The Growing Fisher's Equation accurately models NC cell invasion to form the ENS. The interactions between proliferation, motility and gut growth dictate whether or not colonisation is successful.

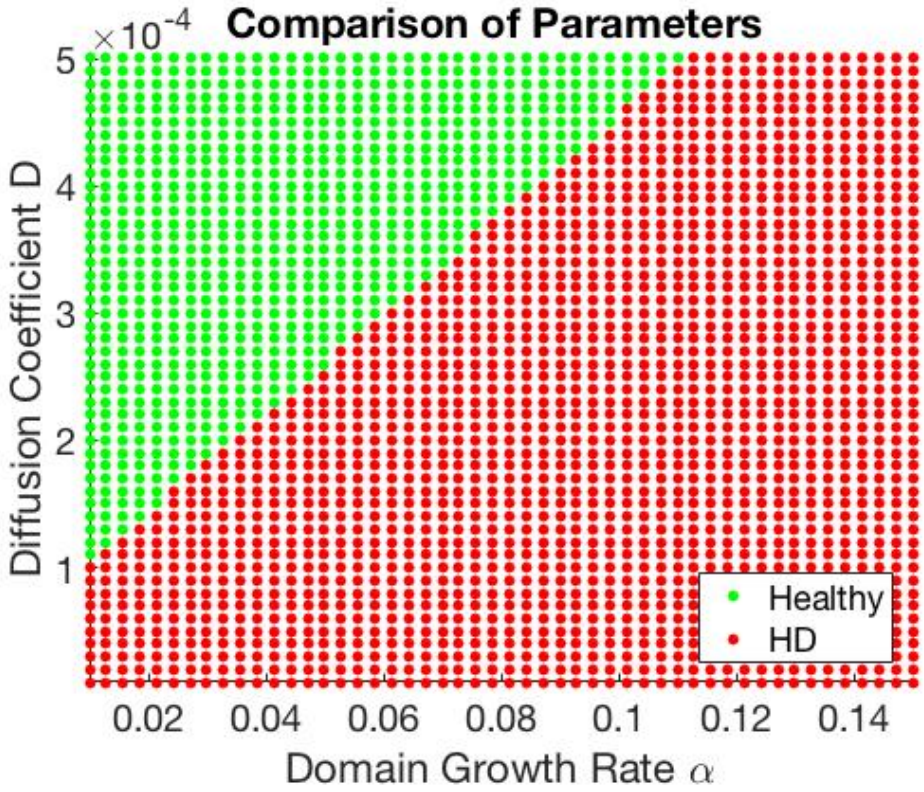

FIGURE 4.6: 2500 simulations of the Growing Fisher's Equation for different values D and α. For healthy individuals (green) means that the travelling wave of NC cell reached the caudal end point of the gut while those with HD (red) the travelling wave of NC cell failed to reach the caudal end point of the gut. The duration of each simulation was $t = 60$

Hirschsprung's disease (HD) occurs when NC cells fail to colonise the distal bowel. In a mathematical context it suggests that D was not sufficiently large enough to over come the domain growth rate α. Therefore, by the end of the simulation one would observe a region of aganglionosis rostral to position $x = L$. In Figures 4.5a, 4.5c and 4.5e the wave fronts do not reach the caudal end of the domain before we terminate the simulation. This is a characteristic of HD.

Previous mathematical investigations of cell colonisation on a growing tissue have illustrated that the interplay between the rate of tissue growth and the initial number of invading cells is critical to determining whether a population of cells can completely colonise a growing tissue [9, 11, 32]. For the models in this thesis, the initial population size is fixed. We investigate the interplay between the cell motility D with the domain growth rate α. Note that due to the choice of scaling the proliferation rate has be incorporated into the scaled diffusion coefficient.

Figure (4.6) compares the diffusion coefficient D with the domain growth rate α. There appears to be a linear threshold between D and α which determines the occurrence of HD. For low diffusion rates and with fast domain growth we see Hirschsprung like features. For high diffusion rates and with slow domain growth we do not see Hirschsprung like features.

Note, the particular form of gut growth is chosen to be exponential. This is because biological investigations discussed in Chapter 3 [20, 33] consider quail guts which undergo rapid elongation over the E4-E6 development period thus implying exponential growth is appropriate.

4.5 Summary

From a simple diffusion model we have successfully constructed a continuum model that describes NC cell invasion to form the ENS. This was achieved by adding a reaction and an advection term to the diffusion model. This yielded the Growing Fisher's Equation,

$$\frac{\partial u}{\partial t} = \underbrace{D\frac{\partial^2 u}{\partial x^2}}_{\text{Motility}} + \underbrace{ku\left(1-\frac{u}{C}\right)}_{\text{Proliferation}} - \underbrace{\frac{\partial (vu)}{\partial x}}_{\text{Gut Growth}} .$$

Our model was solved using the MOL in combination with a domain fixing technique to remove hyperbolic terms. Finally, we compared the diffusion coefficient with the domain growth rate to understand how occurrence of HD was influenced. The simulations revealed that with lower diffusion rates with fast domain growth will give rise to Hirschsprung like features.

Chapter 5

A Model for Skip Segment Hirschsprung Disease

In this chapter a mathematical model for the phenomenon, skip segment Hirschsprung disease (SSDH) is developed. Following this we outline a computational method to find numerical solutions of the proposed mathematical model. Then finally, we will investigate the contributions certain skipping parameters contribute to invasion.

5.1 Model Development

5.1.1 Biological Assumptions

Before proceeding into rigorous mathematical and computational development of our model, we outline some biological definitions, assumptions and simplifications.

SSHD is characterised by a 'skip area' of normally ganglionated intestine, surrounded by aganglionosis. The skipping phenomenon we model has no clear embryological explanation [3]. In order to proceed with a reasonable mathematical model

we assume that a skip segment occurs when NC cells from a region of the rostral ganglionated intestine diffuse into the caudal aganglionic intestine. Therefore two small cultures of cells invade the ENS. Under these assumptions, failure to colonise the gut during the development of the fetus in the mother's womb will result in SSHD. Also it should be noted that the segment of the population that skipped to the more caudal region is allowed to invade both rostro-caudally and caudo-rostrally. Note, that this property maybe biologically impossible due to the affects of GDNF. However, the effects of chemotaxis are not considered in this thesis so to be mathematically consistent we permit rostro-caudal and caudo-rostral invasion.

5.1.2 Mathematical Description

From a mathematical perspective, the model we develop must capture the skip details outlined above while preserving all the properties of NC cell invasion discussed in Chapter 4. Introducing a skip into the model for NC cell invasion is done in a similar vein as reaction was added to the diffusion equation or advection was added to Fisher's Equation. Simply add a skipping term to the governing equation. In words this is

Cell Invasion

$$= \textbf{Cell Motility} + \textbf{Cell Proliferation} + \textbf{GutGrowth} + \textbf{Cell Skipping}.$$

However, before outlining what the skipping term is we will introduce some notation.

First, we adopt indicator functions defined as

$$\mathbf{1}_{x\in[a,b]} := \begin{cases} 1 & x \in [a,b] \\ 0 & \text{otherwise} \end{cases}$$

where $a, b \in \mathbb{R}$. Equivalently, Heaviside functions could have been employed. However, indicator functions are preferred since they are more compact and easier to translate into code.

Mathematically, a skip means that the cell density u at position x will need to depend on points which lie in the opposite region of the domain. Thus, we let

$$u^{(\gamma)} := u(x+\gamma, t), \quad u^{(-\gamma)} := u(x-\gamma, t)$$

this is the cell density evaluated at position $x+\gamma$ and $x-\gamma$ respectively.

Lastly we will define, new parameters that correspond to the new skipping term. We let

- $S_1(t)$ = the left boundary of the rostral skipping segment,
- $S_2(t)$ = the left boundary of the caudal skipping segment,
- $S(t)$ = the length of both skips,
- $P(t) = S_2(t) - S_1(t)$ = the distance a cell skips if it happens to skip,
- t_1 = the time the skip commences,
- τ = the duration of the skip.

All location parameters $(S_1(t), S_2(t), S(t), P(t))$ are functions of time due to the growth of the domain. Later, we use the domain fixing technique from Chapter 4 to remove the time dependence. Figure 5.1 shows the location of each spacial parameter.

Now that all new parameters have been defined we are now in a position to state the skipping term explicitly. We propose that

$$\text{Cell skipping} = k\Big[(1-u)u^{(P)} - (1-u^{(P)})u\Big]\mathbf{1}_{x\in[S_1(t),S_1(t)+S(t)]}\mathbf{1}_{t\in[t_1,t_1+\tau]} \tag{5.1}$$
$$+\, k\Big[(1-u)u^{(-P)} - (1-u^{(-P)})u\Big]\mathbf{1}_{x\in[S_2(t),S_2(t)+S(t)]}\mathbf{1}_{t\in[t_1,t_1+\tau]}$$

where k is the usual mitotic index associated with cell proliferation. Equation (5.1) is only active during times $t \in [t_1, t_1 + \tau]$. The first term in (5.1) represents proliferation of NC cells for $x \in [S_1(t), S_1(t) + S(t)]$ to a carrying capacity, which depends on the density of cells at $x+P(t)$. This can be thought of as the inflow of cells into the segment $[S_1, S_1 + S]$.

The second term in (5.1) represents the death of NC cells for $x \in [S_1(t), S_1(t)+S(t)]$ which depends on the density of cells at $x + P(t)$. This is the outflow of cells from the segment $[S_1(t), S_1(t) + S(t)]$.

The third term in (5.1) represents proliferation of NC cells for $x \in [S_2(t), S_2(t)+S(t)]$ to a carrying capacity, which depends on the density of cells at $x - P(t)$. This can be thought of as the inflow of cells into the segment $[S_2(t), S_2(t) + S(t)]$.

The fourth term in (5.1) represents the death of NC cells for $x \in [S_2(t), S_2(t)+S(t)]$ which depends on the density of cells at $x - P(t)$. This is the outflow of cells from the segment $[S_2(t), S_2(t) + S(t)]$.

In a similar manner to the reaction term, the skipping term adopts a logistic growth model. This type of model is important since it prevents local over-saturation of the cell density. That is $0 \leq u \leq 1$ for $x \in [S_1(t), S_1(t) + S(t)] \cup [S_2(t), S_2(t) + S(t)]$.

Lastly, (5.1) has an intrinsic symmetry in the spacial variable x. This gives our model the property of reversibility. Biologically, only cells cultures of higher densities will diffuse into areas with lower or zero cell densities. More simply, the direction of

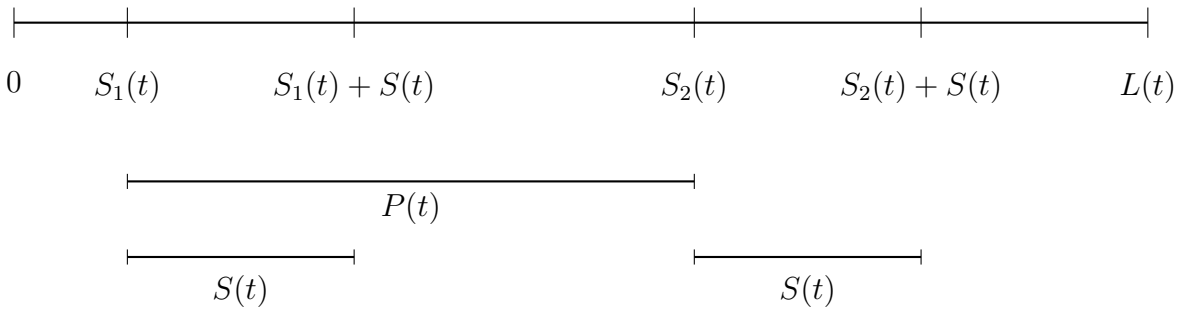

FIGURE 5.1: A representation of the gut displaying the physical locations of the spacial parameters in the proposed mathematical model.

the skip is dependent on cell density.

Adding (5.1) to the Growing Fisher's Equation (4.12) from Chapter 4 we find that the appropriate continuum model is

$$\begin{aligned}\frac{\partial u}{\partial t} &= D\frac{\partial^2 u}{\partial x^2} + ku(1-u) - \frac{\partial (vu)}{\partial x} \\ &\quad + k\Big[(1-u)u^{(P)} - (1-u^{(P)})u\Big]\mathbf{1}_{x\in[S_1(t),S_1(t)+S(t)]}\mathbf{1}_{t\in[t_1,t_1+\tau]} \\ &\quad + k\Big[(1-u)u^{(-P)} - (1-u^{(-P)})u\Big]\mathbf{1}_{x\in[S_2(t),S_2(t)+S(t)]}\mathbf{1}_{t\in[t_1,t_1+\tau]}.\end{aligned} \tag{5.2}$$

Scaling our model is done by introducing the same dimensionless variables from the Growing Fisher's Equation [9, 10],

$$x^* = \frac{x}{L_0}, \quad t^* = kt, \quad v^* = \frac{v}{\lambda L_0}, \tag{5.3}$$

and we have the dimensionless parameters,

$$D^* = \frac{D}{kL_0^2}, \quad L^* = \frac{L}{L_0}. \tag{5.4}$$

These are the exactly the parameters from Chapter 4. However because we have introduced a skip we also have dimensionless parameters corresponding to the skip term,

$$S(t)^* = \frac{S(t)}{L_0}, \quad S_1(t)^* = \frac{S_1(t)}{L_0}, \quad S_2(t)^* = \frac{S_2(t)}{L_0}, \quad t_1^* = kt_1, \quad \tau^* = k\tau.$$

This leads to the following dimensionless system (where the asterisks have been discarded for notational simplicity),

$$\begin{aligned}\frac{\partial u}{\partial t} &= \frac{\partial^2 u}{\partial x^2} + u(1-u) - \frac{\partial (vu)}{\partial x} \\ &+ \left[(1-u)u^{(P)} - (1-u^{(P)})u\right]\mathbf{1}_{x\in[S_1(t),S_1(t)+S(t)]}\mathbf{1}_{t\in[t_1,t_1+\tau]} \\ &+ \left[(1-u)u^{(-P)} - (1-u^{(-P)})u\right]\mathbf{1}_{x\in[S_2(t),S_2(t)+S(t)]}\mathbf{1}_{t\in[t_1,t_1+\tau]}.\end{aligned} \tag{5.5}$$

For computational simplicity the domain is fixed on $[0,1]$ for all $t \geq 0$, [9, 10]. This is done by introducing

$$\xi = \frac{x}{L(t)},$$

thus yielding

$$\begin{aligned}\frac{\partial u}{\partial t} &= \frac{D}{L^2}\frac{\partial^2 u}{\partial \xi^2} + u(1-u) - u\frac{1}{L}\frac{dL}{dt} \\ &+ \left[(1-u)u^{(P/L)} - (1-u^{(P/L)})u\right]\mathbf{1}_{\xi\in\left[\frac{S_1}{L},\frac{S_1+S}{L}\right]}\mathbf{1}_{t\in[t_1,t_1+\tau]} \\ &+ \left[(1-u)u^{(-P/L)} - (1-u^{(-P/L)})u\right]\mathbf{1}_{\xi\in\left[\frac{S_2}{L},\frac{S_2+S}{L}\right]}\mathbf{1}_{t\in[t_1,t_1+\tau]}\end{aligned} \tag{5.6}$$

where $L := L(t) = e^{\alpha t}$ meaning that the gut growth is exponential with rate α. This type of domain growth is chosen because it models gut growth better than a linear or a logistic model during the the E4-E6 period in quail embryos [43]. Refer back to the Chapter 2 for a full justification. The reader should also note that

$$\frac{1}{L}\frac{dL}{dt} = \alpha = \text{constant}$$

and since $S_1(t), S_2(t)$ and $S(t)$ vary with t in exactly the same way $L(t)$ varies with t,

$$\frac{S_1(t)}{L(t)}, \quad \frac{S_1(t)+S(t)}{L(t)}, \quad \frac{S_2(t)}{L(t)}, \quad \frac{S_2(t)+S(t)}{L(t)},$$

are constants after fixing the domain.

5.1.3 Computational Model

Fixing the domain removes the hyperbolic terms from Equation (5.5) so we can use the MOL routine to solve Equation (5.6).

First, the fixed spacial domain is discretised into $x_1, x_2, \ldots, x_{N+1}$ with N intervals. Each interval has step size $h = 1/N$.

Computationally a skip implies that diffusion at x_i will not only depend on x_{i-1} and x_{i+1} but will also depend on some point x_{i+p} where p represents some number of mesh points from mesh point i. In order to be consistent with the mathematical notation above we define,

$$p := \frac{P}{hL},$$

and so

$$s_1 := \frac{S_1}{hL}, \quad s_2 := \frac{S_2}{hL}, \quad s := \frac{S}{hL}.$$

There is a factor of $1/L$ in the above definitions because all numerical simulations are solved on the fixed domain. Before we state the computational model explicitly for brevity we define the following.

$$\mathbf{U} = \underbrace{\begin{bmatrix} u_1 \\ \vdots \\ \\ \\ \\ \vdots \\ u_{N+1} \end{bmatrix}}_{(N+1)\times 1}, \quad \dot{\mathbf{U}} = \underbrace{\begin{bmatrix} du_1/dt \\ \vdots \\ \\ \\ \\ \vdots \\ du_{N+1}/dt \end{bmatrix}}_{(N+1)\times 1}, \quad \mathbf{M} = \underbrace{\begin{bmatrix} -2 & 2 & & & & & & & \\ 1 & -2 & 1 & & & & & & \\ & \ddots & \ddots & \ddots & & & & & \\ & & & & & & & & \\ & & & & \ddots & \ddots & \ddots & & \\ & & & & & 1 & -2 & 1 & \\ & & & & & & 2 & -2 \end{bmatrix}}_{(N+1)\times(N+1)},$$

$$\mathbf{P} = \underbrace{\begin{bmatrix} u_1(1-u_1) \\ \vdots \\ \\ \\ \\ \vdots \\ u_{N+1}(1-u_{N+1}) \end{bmatrix}}_{(N+1)\times 1}, \quad \mathbf{G} = \underbrace{\begin{bmatrix} u_1 L^{-1} dL/dt \\ \vdots \\ \\ \\ \\ \vdots \\ u_{N+1} L^{-1} dL/dt \end{bmatrix}}_{(N+1)\times 1}.$$

Explicitly, the discretisation of Equation (5.6) yields

$$\begin{aligned} \frac{du_i}{dt} &= \frac{u_{i-1} - 2u_i + u_{i+1}}{h^2} + u_i(1-u_i) - u_i \frac{1}{L}\frac{dL}{dt} \\ &+ \Big[(1-u_i)u_{i+p} - (1-u_{i+p})u_i\Big] \mathbf{1}_{\xi_i \in [s_1,(s_1+s)]} \mathbf{1}_{t\in[t_1,t_1+\tau]} \\ &+ \Big[(1-u_i)u_{i-p} - (1-u_{i-p})u_i\Big] \mathbf{1}_{\xi_i \in [s_2,(s_2+s)]} \mathbf{1}_{t\in[t_1,t_1+\tau]}. \end{aligned}$$

In matrix form when $t \in [t_1, t_1+\tau]$ (the skipping is turned on) we have

$$\dot{\mathbf{U}} = \frac{1}{h^2}\mathbf{A}\mathbf{U} + \mathbf{P} - \mathbf{G} + \mathbf{S}_1 - \mathbf{S}_2 + \mathbf{S}_3 - \mathbf{S}_4.$$

We have defined,

$$\mathbf{S}_1 = \underbrace{\begin{bmatrix} \\ u_{s_2}(1-u_{s_1}) \\ \vdots \\ u_{(s_2+s)}(1-u_{(s_1+s)}) \\ \\ \end{bmatrix}}_{(N+1)\times 1}, \quad \mathbf{S}_2 = \underbrace{\begin{bmatrix} \\ u_{s_1}(1-u_{s_2}) \\ \vdots \\ u_{(s_1+s)}(1-u_{(s_2+s)}) \\ \\ \end{bmatrix}}_{(N+1)\times 1}$$

$$\mathbf{S}_3 = \underbrace{\begin{bmatrix} \\ \\ u_{s_1}(1-u_{s_2}) \\ \vdots \\ u_{(s_1+s)}(1-u_{(s_2+s)}) \\ \\ \end{bmatrix}}_{(N+1)\times 1}, \quad \mathbf{S}_4 = \underbrace{\begin{bmatrix} \\ \\ u_{s_2}(1-u_{s_1}) \\ \vdots \\ u_{(s_2+s)}(1-u_{(s_1+s)}) \\ \\ \end{bmatrix}}_{(N+1)\times 1}.$$

$\mathbf{S}_1$ and $\mathbf{S}_2$ have non-zero elements between indices $[s_1, s_1 + s]$ while $\mathbf{S}_3$ and $\mathbf{S}_4$ have non-zero elements between indices $[s_2, s_2 + s]$.

5.2 Model Implementation and Simulation

In this section we will perform an in silico experiments with two key objectives. One, reproduce a invasion profile that is typical of SSHD. Two, investigate how the interactions between parameters affect invasion.

There is already a large body of literature that investigates the interaction and contributions between the diffusion coefficient, proliferation rate and gut growth rate [9, 10, 11, 32, 43]. We are more interested in the parameters corresponding to the skipping term from Equation (5.6). Table 5.1 lists the skipping parameters, their role each will play in NC cell invasion and their assigned default values for the upcoming *in silico* experiments. Default values are chosen such that the invasion profile resembles SSHD.

In this chapter the term HD will mean that there exists one segment of aganglionosis between the initial population of cells and the caudal end point of the gut L (Figure 5.2b). A skip will mean that there is only a segment of aganglionosis between the initial population of cells and the skipped population of cells (Figure 5.2c). SSHD or HD with a skip will mean that there are two segments of aganglionosis. The first is between the initial population of cells and skipped population of cells segment. The second is between the skipped population and L (Figure 5.2d).

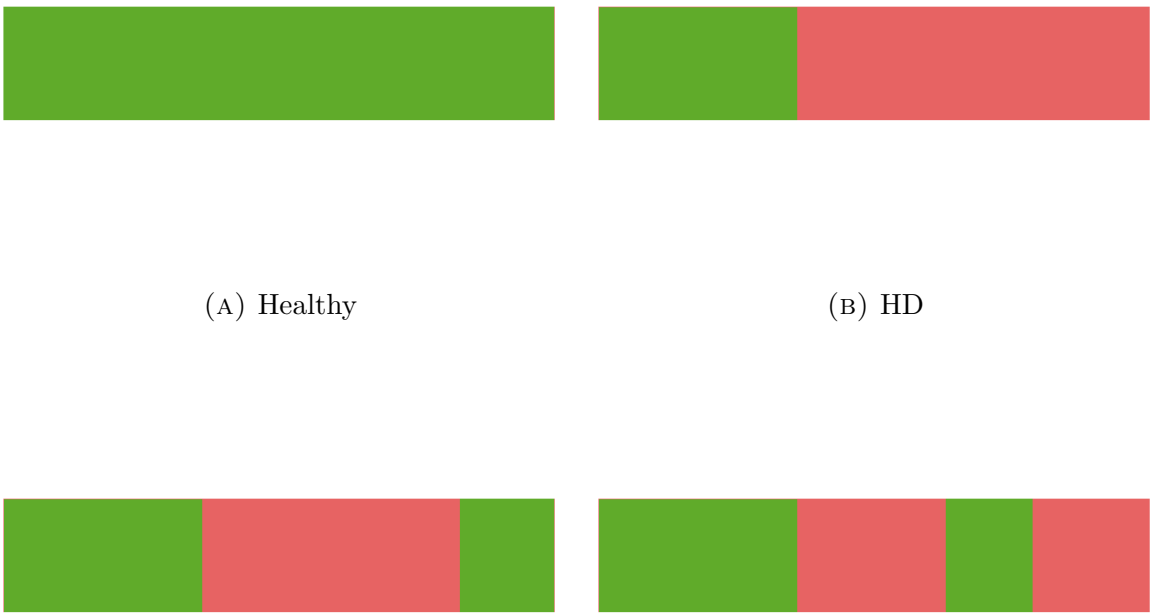

(A) Healthy (B) HD

(C) Skip only (D) SSHD or HD with a skip

FIGURE 5.2: Outcomes of invasion. Green areas represent successful NC invasion. Dark pink areas represent unsuccessful NC invasion.

Parameter	Description	Default Value
D	Diffusion coefficient.	0.00001
α	Gut growth rate.	0.1
S_1	Left end point of the rostral skip segment.	0.1
S_2	Left end point of the caudal skip segment.	0.6
S	The length of each segment.	0.1
P	The distance a cell skips.	0.5
t_1	Skip start time.	20
τ	The duration of the skip.	10

TABLE 5.1: A table of all parameters (after scaling), with a brief description and their default values.

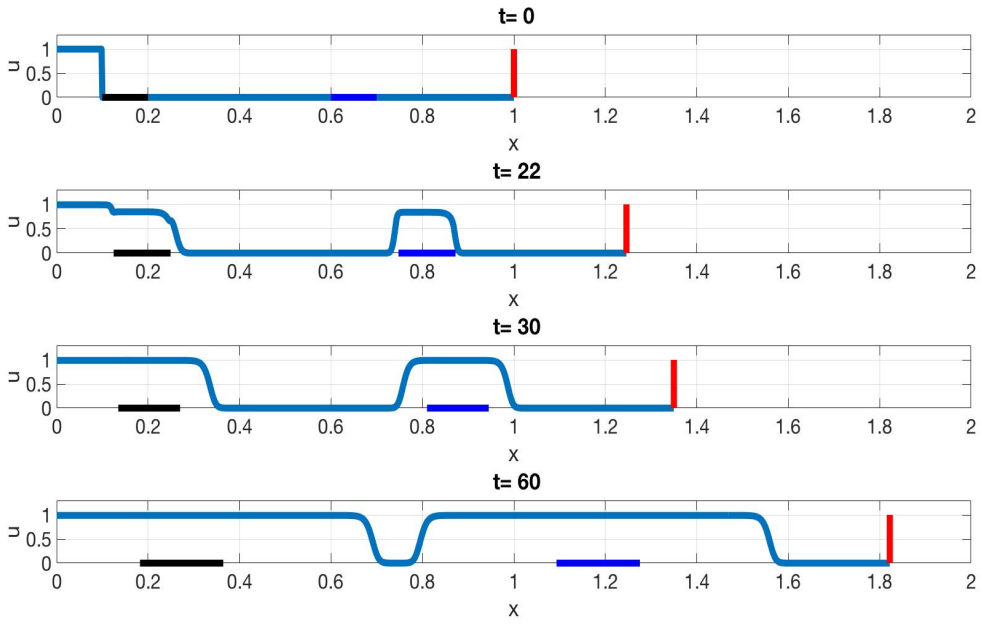

FIGURE 5.3: An invasion profile illustrating SSHD. Parameters for this simulation can be found in Table 5.1.

5.2.1 A Typical Skip Segment Profile

From the default values listed in Table 5.1 we generate an invasion profile (Figure 5.3) and the corresponding characteristic curves (Figure 5.4) corresponding to a case of SSHD. Note that all quantities presented in this chapter are dimensionless but unfixed in the spacial domain. Using the domain fixing technique only makes the numerical solution easier to compute so for sake of interpretability the domain is unfixed in all figures.

From Figure 5.3 NC cells invade rostro-caudally. Once the population reaches the rostral skip segment (black) and skipping is turned on (that is $t \in [t, t+\tau]$) cells will skip to the caudal skip segment (dark blue). Both populations will continue to invade the gut until the simulation is terminated at $t = 60$. Note that the skipped population is allowed to invade rostro-caudally and caudo-rostrally.

From Figure 5.4 we are able to see the complete time evolution of the invasion wave. This is advantageous because even if we did not know what the preset parameter values were we could estimate where and when the skip originated.

5.2.2 Parameter Investigation

Now that we have established base parameter values that produce SSHD we will first vary each parameter separately and then vary pairs of parameters to better understand their contribution to SSHD. In Chapter 4, after we non-dimensionalised, the Growing Fisher's Equation only had two parameters; the diffusion coefficient D and the gut growth rate α. In this chapter even after we non-dimensionalise our model we have an overwhelming total of 8 parameters to investigate. We choose to fix D, α, t_1 and τ and use the fact that $P = S_2 - S_1$ to reduce the number of parameters in our system. Therefore, S_1, S and P will only be examined.

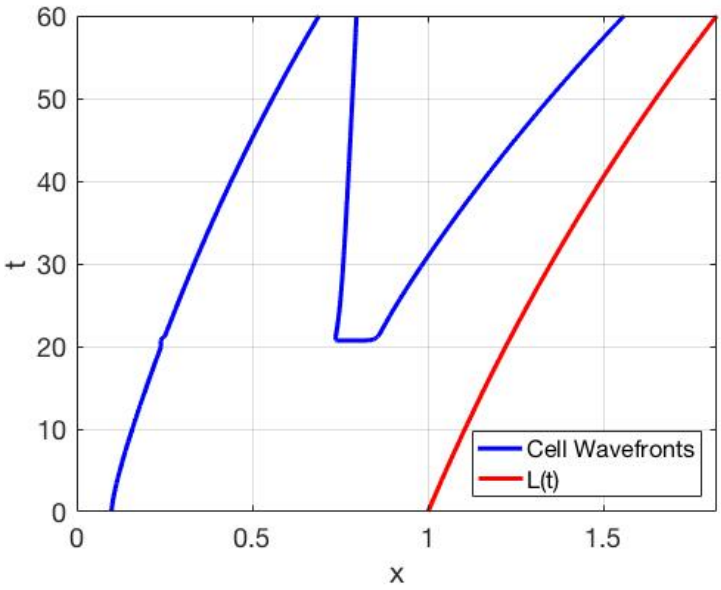

FIGURE 5.4: Characteristic curves for NC cell wavefronts (blue) and the caudal end point $L(t)$ (red). Parameters for this simulation can be found in Table 5.1.

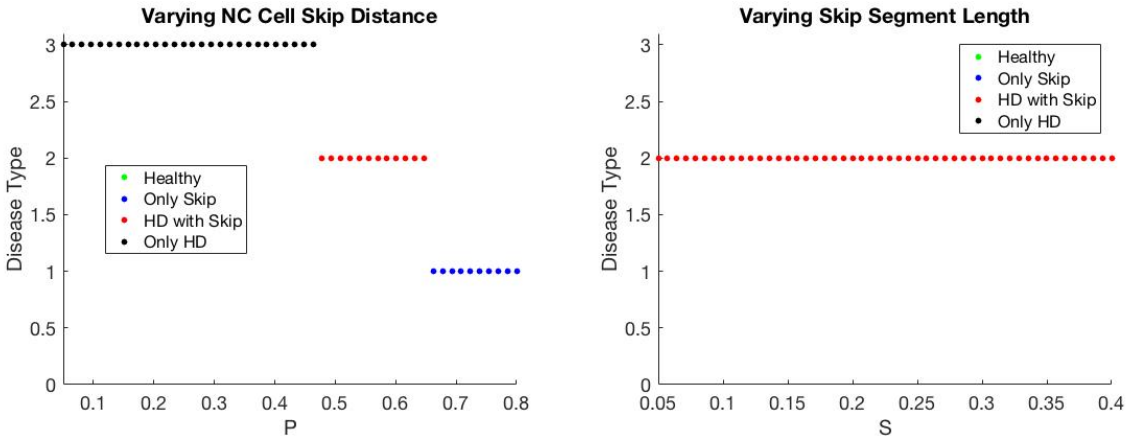

(A)

(B)

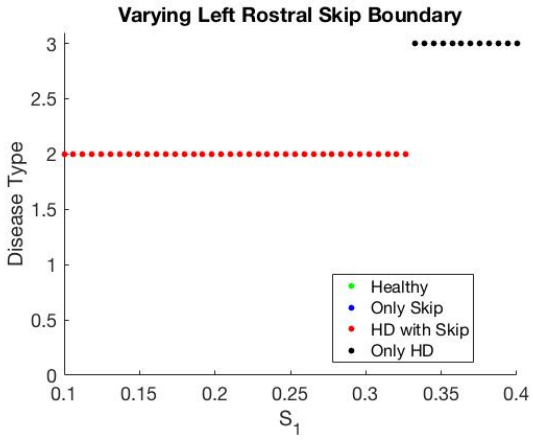

(C)

FIGURE 5.5: One dimensional sweeps of spacial skipping parameters.

We consider four outcomes of the invasion process. One, the subject is completely healthy, that is the NC cell density is one for all $x \in [0, L]$ (green). We remark that in the following simulations there are no healthy outcomes. For the particular choice of default parameters in Table 5.1, healthy outcomes only occur rarely or for non-physical choices of the varied parameters. Two, there is only a skip between two NC cell populations segments (blue). Three, the subject only has HD that is there is only aganglionosis between caudal end point of the gut and the initial population. Four, the subject has both HD and a skip between the two populations of NC cells, similar to what was shown in Figure 5.3 (red).

One parameter sweeps from Figure 5.5 do not provide us with new insights about SSHD but instead confirm that our model accurately describes what is happening biologically. Figure 5.5a shows us what happens when we vary the distance a cell can skip. For increasing P the invasion outcome shifts from HD to HD with a skip then to only a skip. This implies that as P increases more caudal areas are filled before the region of aganglionosis between both populations. Figure 5.5b suggests the invasion outcome is independent of the length of the skip segment as HD with a skip is present for all values of S. However it is more likely that there was an insufficient cell density at the rostral skip segment to warrant an increase in cell skipping just because the skip segment length had increased. For example if we started with a larger initial population or we used a higher diffusion coefficient a greater proportion of cells would be permitted to skip due to a higher value of S.

Figure 5.5c tells us that as S_1 increases an individual could be saved from SSHD and only have HD. For larger values S_1 the NC cell population was not able to invade sufficiently fast enough to reach S_1. Therefore, no skipping occurred which resulted in a region of a between the rostral skip segment and the the caudal gut end point.

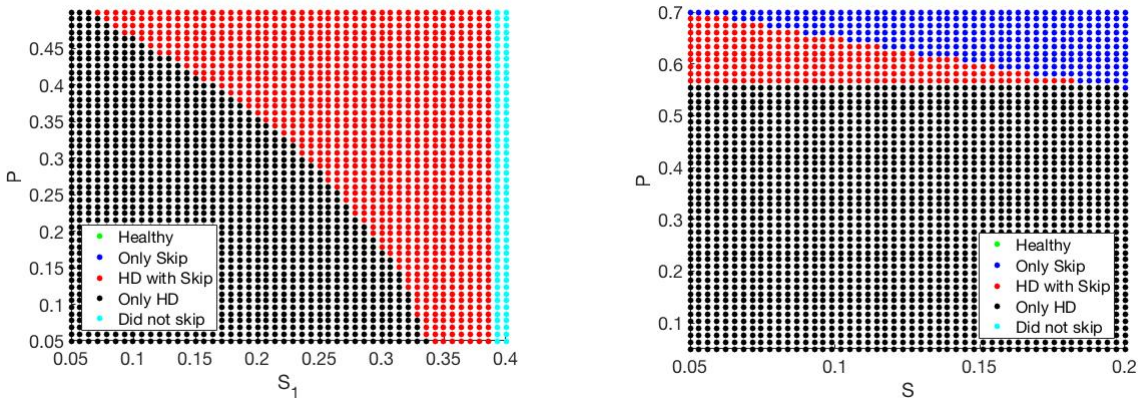

(A) (B)

FIGURE 5.6: A comparison between the spacial skipping parameters in order to understand the occurrence of HD and SSHD.

Next we will investigate the interactions between the skipping parameters and how they contribute to the final invasion outcome. It was observed from Figure 5.5c for large enough values of S_1 the population does not reach the rostral skip segment and there is no skip during that particular simulation. Thus, we will classify this as a separate fifth outcome of invasion. In the Figures 5.6 an invasion that does not skip will be denoted by a cyan dot.

First we seek to understand the relationship between the skipping distance P and the position of the left rostral skip. From Figure 5.6b we observe a non-linear relationship governing the outcome of invasion. For low and high values of P invasion only produces HD. Note that if we considered even higher values of P during our simulation at some large enough P we should begin to see an area of blue representing individuals with a skip. Once P and S_1 cross the non-linear threshold seen in Figure 5.6a invasion produces HD with a skip. However, as illustrated by the cyan columns for some sufficiently large S_1 invasion once again only produces HD since members of the cell population were unable to reach the rostral skip segment.

Next we seek to understand the relationship between the skipping distance P and the length of the skip segments S. For the values we have sampled one can observed that for roughly $P < 0.55$ we only see that HD is the invasion outcome regardless of the value of S. Once $P > 0.55$ there appears to be a set of P such that invasion produces HD with a skip. However, as P and S become large invasion only produces a skip. Physically, cells skip greater distances and so the proportion of cells permitted to skip is greater. Therefore, caudal areas of the gut are more likely to be colonised.

5.3 Summary

In this chapter we have proposed a continuum model for SSHD. Our model adds to the Growing Fisher's Equation by introducing a cell skipping term. Explicitly, the governing PDE is

$$\begin{aligned}\frac{\partial u}{\partial t} = &\underbrace{D\frac{\partial^2 u}{\partial x^2}}_{\text{Motility}} + \underbrace{ku\left(1-\frac{u}{C}\right)}_{\text{Proliferation}} - \underbrace{\frac{\partial(vu)}{\partial x}}_{\text{Gut Growth}} \\ &+ \underbrace{k\left[(1-u)u^{(P)} - (1-u^{(P)})u\right]\mathbf{1}_{x\in[S_1(t),S_1(t)+S(t)]}\mathbf{1}_{t\in[t_1,t_1+\tau]}}_{\text{Skipping}} \\ &+ \underbrace{k\left[(1-u)u^{(-P)} - (1-u^{(-P)})u\right]\mathbf{1}_{x\in[S_2(t),S_2(t)+S(t)]}\mathbf{1}_{t\in[t_1,t_1+\tau]}}_{\text{Skipping}}.\end{aligned}$$

Following this we outlined a numerical algorithm that solved the above PDE. Finally we assigned default parameter values that produced SSHD and investigated the contributions certain skipping parameters made to invasion.

Chapter 6

Discussion and Conclusion

This thesis aimed to mathematically model SSHD. In this chapter we will review the content of the thesis and discuss the biological conclusions from Chapter 4 and Chapter 5. Then we close by outlining possible directions for future work.

6.1 Thesis Summary

Chapter 2 provided the reader with all the necessary biological preliminaries about the ENS to better contextualise the proceeding mathematical models.

Chapter 3 outlined the biological and mathematical discoveries corresponding to the ENS. From these discoveries one could describe NC cell colonisation by the following three rules [47]. One, NC cell motility is unidirectional. That is vagal NC cells invade rosto-caudally while sacral NC cells migrate caudo-rostrally. Two, NC cells proliferate up to an intestinal carrying capacity. Three, intestinal growth influences NC cell invasion. Interactions between these three rules can be qualitatively described by a word equation,

$$\textbf{Cell Invasion} = \textbf{Cell Motility} + \textbf{Cell Proliferation} + \textbf{Gut Growth}.$$

It was noted that one could model NC cell invasion using either CA models or continuum models. CA models provide information about the NC cell population and also individual NC cells while the continuum model only provides information about the population. However, the advantage a continuum model has over a CA model is that it is computationally faster. In Chapter 4 we chose to use continuum models. First, we considered a simple diffusion model that represented cell motility. Next, we added cell proliferation to our model by considering the Fisher's Equation. Finally, incorporated gut growth by considering an advection-reaction-diffusion equation which we called the Growing Fisher's Equation. This is given by

$$\frac{\partial u}{\partial t} = \underbrace{D\frac{\partial^2 u}{\partial x^2}}_{\text{Motility}} + \underbrace{ku\left(1-\frac{u}{C}\right)}_{\text{Proliferation}} - \underbrace{\frac{\partial (vu)}{\partial x}}_{\text{Gut Growth}} .$$

For each model we obtained a numerical solution using the MOL algorithm. The diffusion model has an exact solution so we were able to check our numerical solution with the exact solution to ensure accuracy. Fisher's Equation unfortunately does not have a general closed form solution so we compared the numerically computed wave speed with the theoretical wave speed. For the growing Fisher's Equation both a closed form solution and the theoretical wave speed have not been found in the literature. However, since our numerical solution for the diffusion model and Fisher's Equation both supported theoretical results mentioned above its not unreasonable to assume that the MOL algorithm produced an accurate numerical solution for the Growing Fisher's Equation. Following this, different types of domain growth were investigated. Lastly, we showed how the Growing Fisher's Equation can model the occurrence of HD. After some parameter investigation we showed that there is a linear threshold in the parameter space which determines the occurrence of HD.

In Chapter 5 a model for SSHD was constructed by adding a cell skipping term to the Growing Fisher's Equation. This gave the continuum model,

$$\begin{aligned}\frac{\partial u}{\partial t} = & \underbrace{D\frac{\partial^2 u}{\partial x^2}}_{\text{Motility}} + \underbrace{ku\left(1-\frac{u}{C}\right)}_{\text{Proliferation}} - \underbrace{\frac{\partial (vu)}{\partial x}}_{\text{Gut Growth}} \\ & \underbrace{+ k\left[(1-u)u^{(P)} - (1-u^{(P)})u\right]\mathbf{1}_{x\in[S_1(t),S_1(t)+S(t)]}\mathbf{1}_{t\in[t_1,t_1+\tau]}}_{\text{Skipping}} \\ & \underbrace{+ k\left[(1-u)u^{(-P)} - (1-u^{(-P)})u\right]\mathbf{1}_{x\in[S_2(t),S_2(t)+S(t)]}\mathbf{1}_{t\in[t_1,t_1+\tau]}}_{\text{Skipping}}.\end{aligned} \tag{6.1}$$

Again, we applied the MOL to solve the proposed model. Then we examined how various parameters interacted to affect the invasion outcome. That is if the invasion profile has segments of zero NC cell density which biologically correspond to and individual with HD or SSHD.

6.2 Biological Implication

The results presented in Chapter 4 and Chapter 5 provide interesting biological interpretations about HD and SSHD respectively.

Computer simulations of the Growing Fisher's Equation showed that cell motility and cell proliferation compete against the gut growth to colonise the ENS. If the gut growth is so fast that the NC wavefront cannot reach the caudal end point of the gut the individual would present with HD.

Next the model for SSHD was introduced. The skipping term in Equation (6.1) contained five new parameters associated with the dynamics of the skip. Having this many parameters in the model gives one the freedom to easily engineer invasion so a

specific outcome is achieved. For example a case report by Ruiz *et al.* [3] qualitatively describes a patient with SSHD. Hence, a careful choice of parameters could match the observation made by Ruiz *et al.* [3]. No quantitative data about SSHD was found in the literature so an exact matching of a simulated invasion profile with biological observations was not possible.

Chapter 5 closed with an investigation of the spacial skipping parameters. From the two parameter experiment the skipping distance P was compared with the position of the rostral skip S_1 (specifically the left boundary of the rostral skip) and the length of the skip S. In both cases it was shown that as the skipping distance increases the outcome of invasion moves from HD to SSHD to only a skip. A reasonable explanation is that for low P the initial population and the skipped population were close to each other so the aganglionic region between populations was fully colonised. However, for larger P the aganglionic region between populations was so large that it was not colonised by the time invasion was terminated.

6.3 Future Work

This thesis has presented the first steps towards a mathematical model of SSHD. In this section, we discuss possible directions for future work. These include modelling using the CA approach, relaxation of the uniform growth assumption, further investigation of the model parameters, chemotaxis and some investigation about inferring the origin of a skip given the final invasion profile.

6.3.1 Using a CA Model

In addition to a population overview a CA model would also provide information about individual cells. Knowing information about individual cells may provide insights about which NC cells were responsible for the skip or inferences about the origin of a skip given a final invasion profile.

Further Parameter Investigation

In Chapter 5 the only parameters we varied were S_1, S and P. These parameters store spacial information about a skip. However our model had a total of seven independent parameters. A more complete study should investigate how temporal parameters t_1 and τ and also invasion parameters D and α interact with each other and the spacial parameters.

Relaxing Uniform Growth Assumption

It has been well document in the biological literature that the gut does not elongate uniformly [43, 20]. The growth rate of the foregut and midgut have been shown to be almost twice as fast as the growth rate for the hindgut. Simpson *et al.* [10] have successfully constructed an algorithm that take non-uniform growth into account. Therefore if one wanted, non-uniform growth affects may be incorporated into the SSHD model.

Chemotaxis

GDNF is a known chemoattractant for NC cells [25]. Therefore it has been suggested that the unidirectional movement of NC cells are due to the influence of GDNF [25]. In

their paper on non-uniformly growing domains, Simpson *et al.* [10] also take into account the affects of chemotaxis. Therefore, in theory this feature could also be combined with the model presented in Chapter 5.

Inferring the Origin of a Skip

It was alluded to earlier that one may ask if it is possible to trace back to the origin of a skip. The characteristics of the Growing Fisher's Equation do not have a closed form. Thus, one may have to enter the realm of data analysis to find reasonable representations for the characteristic curves. Once this is found the origin of a skip could be inferred.

6.4 Conclusion

We have presented a continuum model for NC cell invasion with a skip that was built from a continuum model without a skip. All continuum models were numerically solved using the MOL algorithm. This model provided mathematical and biological insights into the occurrence of SSHD. From the parameter investigation it can be concluded that as the position of a skip becomes more caudal the invasion outcome transitions from HD to SSHD to only a skip. Further investigation may be perform to understand how temporal parameters affect the invasion outcome. The mathematical models presented in this thesis may be extended to further investigate chemotaxis and non-uniform growth. It also provided a foundation to estimate skip origins.

Appendix A

Analytic Solution of the Diffusion Equation

We are required to solve,

$$\frac{\partial u}{\partial t} = \frac{\partial^2 u}{\partial x^2}, \tag{A.1}$$

with no flux boundary conditions and initial condition

$$u(x, 0) = \cos(\pi x).$$

Seeking a solution of the form

$$u(x, t) = X(x)T(t),$$

we find from Equation (A.1) that

$$\frac{X''(x)}{X(x)} = \frac{T'(t)}{T(t)} = -c^2,$$

where c is some constant. Solving for $X(x)$ and applying the left boundary condition we get

$$X(x) = A\cos(cx),$$

where A is constant. Applying the right boundary condition we have

$$c = n\pi \quad \text{for} \quad n = 0, 1, 2, \ldots$$

Since we are not interested in the general solution we will find the solution for $n = 1$. Solving for $T(t)$ we find

$$T(t) = Be^{-\pi^2 t},$$

where B is some constant. Letting $Q = AB$, a solution of Equation (A.1) is

$$u(x,t) = Q\cos(\pi x)e^{-\pi^2 t}.$$

Lastly, by applying the initial conditions it can be shown that $Q = 1$, so

$$u(x,t) = \cos(\pi x)e^{-\pi^2 t}.$$

Appendix B

The Relationship between the Domain Length and the Domain Velocity.

We must show,

$$\frac{dL}{dt} = \int_0^L \frac{\partial v}{\partial x} dx, \tag{B.1}$$

where $L = L(t)$ is the length of the domain and $v = v(x,t)$ is the velocity of the domain.

First, partition the domain into $0 = x_0 < x_1 \cdots < x_n = L(t)$ and set

$$\Delta x_i = x_i - x_{i-1},$$

so that

$$L(t) = \sum_j \Delta x_j(t), \quad L(t+s) = \sum_j \Delta x_j(t+s).$$

Now,

$$\begin{aligned}\frac{L(t+s)-L(t)}{\Delta t} &= \sum_j \frac{\Delta x_j(t+s)-\Delta x_j(t)}{\Delta t} \\ &= \sum_j \frac{v(x_j(t+s),t+s)\Delta t - v(x_j(t),t)\Delta t}{\Delta t} \\ &= \sum_j \left[v(x_j(t+s),t+s)-v(x_j(t),t)\right],\end{aligned}$$

taking the limit as $\Delta t \to 0$,

$$\frac{dL}{dt} = \int_0^L dv(x,t),$$

and so

$$\frac{dL}{dt} = \int_0^L \frac{\partial v}{\partial x} dx.$$

Appendix C

Domain Fixing for the Growing Fisher's Equation

We that must show that

$$\frac{\partial u}{\partial t} = D\frac{\partial^2 u}{\partial x^2} + u\left(1-u\right) - \frac{\partial (vu)}{\partial x}, \tag{C.1}$$

can by expressed as

$$\frac{\partial u}{\partial t} = \frac{D}{L^2}\frac{\partial^2 u}{\partial \xi^2} + u\left(1-u\right) - u\frac{1}{L}\frac{dL}{dt}. \tag{C.2}$$

under the transformation $\xi = x/L$.

First expand the hyperbolic (last) term in Equation (C.1),

$$\frac{\partial u}{\partial t} + v\frac{\partial u}{\partial x} = D\frac{\partial^2 u}{\partial x^2} + u\left(1-u\right) - u\frac{\partial v}{\partial x}, \tag{C.3}$$

if we consider the transformation

$$(\xi, \bar{t}) = \left(\frac{x}{L(t)}, t\right),$$

by the chain rule it implies

$$\frac{\partial u}{\partial t} = \frac{\partial u}{\partial \bar{t}} + \frac{\partial u}{\partial \xi}\frac{\partial \xi}{\partial \bar{t}},$$

thus

$$\frac{\partial u}{\partial \bar{t}} = \frac{\partial u}{\partial \bar{t}} - \frac{\partial u}{\partial \xi}\frac{x}{L^2}\frac{dL}{d\bar{t}},$$

so

$$\frac{\partial u}{\partial t} = \frac{\partial u}{\partial \bar{t}} - \frac{\partial u}{\partial \xi}\frac{v}{L},$$

using this result and applying the transformation to Equation (C.3),

$$\frac{\partial u}{\partial \bar{t}} = \frac{D}{L^2}\frac{\partial^2 u}{\partial \xi^2} + u\left(1-u\right) - u\frac{1}{L}\frac{dL}{d\bar{t}}, \tag{C.4}$$

dropping the bar notation will yield Equation (C.2).

Bibliography

[1] O. Swenson. "Hirschsprung's disease: a review". In: *Pediatrics* 109.5 (2002), pp. 914–918.

[2] A. O'Donnell and P. Puri. "Skip segment Hirschsprung's disease: a systematic review". In: *Pediatric Surgery International* 26.11 (Nov. 2010), pp. 1065–1069.

[3] S. L. Ruiz et al. "Skip segment Hirschsprung's disease in a patient with Shah-Waardenburg Syndrome". In: *Journal of Pediatric Surgery Case Reports* 15 (2016), pp. 44–47.

[4] D. Silverthorn et al. *Human Physiology: An Integrated Approach*. Pearson Education, 2013. ISBN: 9780321750075.

[5] E. A. Wehrwein, H. S. Orer, and S. M. Barman. "Overview of the anatomy, physiology, and pharmacology of the autonomic nervous system". In: *Comprehensive Physiology* 6.3 (2011), pp. 1239–1278.

[6] J. B. Furness. "The enteric nervous system and neurogastroenterology". In: *Nature reviews Gastroenterology & Hepatology* 9.5 (2012), p. 286.

[7] C. Yntema and W. Hammond. "The origin of intrinsic ganglia of trunk viscera from vagal neural crest in the chick embryo". In: *Journal of Comparative Neurology* 101.2 (1954), pp. 515–541.

[8] R. Anderson, D. Newgreen, and H. Young. "Neural crest and the development of the enteric nervous system". In: *Neural crest induction and differentiation*. Springer, 2006, pp. 181–196.

[9] K. A. Landman, G. J. Pettet, and D. F. Newgreen. "Mathematical models of cell colonization of uniformly growing domains". In: *Bulletin of Mathematical Biology* 65.2 (2003), pp. 235–262.

[10] M. J. Simpson, K. A. Landman, and D. Newgreen. "Chemotactic and diffusive migration on a nonuniformly growing domain: numerical algorithm development and applications". In: *Journal of Computational and Applied Mathematics* 192.2 (2006), pp. 282–300.

[11] M. J. Simpson et al. "Looking inside an invasion wave of cells using continuum models: Proliferation is the key". In: *Journal of Theoretical Biology* 243.3 (2006), pp. 343–360.

[12] G. C. Schoenwolf et al. *Larsen's human embryology E-book*. Elsevier Health Sciences, 2014.

[13] W. W. Zuelzer and J. L. Wilson. "Functional intestinal obstruction on a congenital neurogenic basis in infancy". In: *American Journal of Diseases of Children* 75.1 (1948), pp. 40–64.

[14] W. His. *Untersuchungen über die erste Anlage des Wirbelthierleibes: die erste Entwickelung des Hühnchens im Ei*. Vol. 1. FCW Vogel, 1868.

[15] E. van Campenhout. "Historical Survey of the Development of the Sympathetic Nervous System". In: *Quarterly Review of Biology* 5.1 (1930), pp. 23–50.

[16] N. M. Le Douarin and M.-A. Teillet. "The migration of neural crest cells to the wall of the digestive tract in avian embryo". In: *Development* 30.1 (1973), pp. 31–48.

[17] I. J. Allan and D. F. Newgreen. "The origin and differentiation of enteric neurons of the intestine of the fowl embryo". In: *American Journal of Anatomy* 157.2 (1980), pp. 137–154.

[18] H. D. Pomeranz and M. D. Gershon. "Colonization of the avian hindgut by cells derived from the sacral neural crest". In: *Developmental Biology* 137.2 (1990), pp. 378–394.

[19] W. Webster. "Embryogenesis of the enteric ganglia in normal mice and in mice that develop congenital aganglionic megacolon". In: *Development* 30.3 (1973), pp. 573–585.

[20] D. F. Newgreen et al. "Migration of enteric neural crest cells in relation to growth of the gut in avian embryos". In: *Acta Anatomica* 157.2 (1996), pp. 105–115.

[21] H. Young et al. "A single rostrocaudal colonization of the rodent intestine by enteric neuron precursors is revealed by the expression of Phox2b, Ret, and p75 and by explants grown under the kidney capsule or in organ culture". In: *Developmental biology* 202.1 (1998), pp. 67–84.

[22] A. J. Burns. "Migration of neural crest-derived enteric nervous system precursor cells to and within the gastrointestinal tract". In: *International Journal of Developmental Biology* 49.2–3 (2003), pp. 143–150.

[23] C. J. Hearn, M. Murphy, and D. Newgreen. "GDNF and ET-3 Differentially Modulate the Numbers of Avian Enteric Neural Crest Cells and Enteric Neuronsin Vitro". In: *Developmental biology* 197.1 (1998), pp. 93–105.

[24] D. Natarajan et al. “Multipotential progenitors of the mammalian enteric nervous system capable of colonising aganglionic bowel in organ culture”. In: *Development* 126.1 (1999), pp. 157–168.

[25] H. M. Young et al. “Dynamics of neural crest-derived cell migration in the embryonic mouse gut”. In: *Developmental Biology* 270.2 (2004), pp. 455–473.

[26] J. D. Murray. “Mathematical Biology I. An Introduction”. In: *Springer* (1989).

[27] R. A. Fisher. “The wave of advance of advantageous genes”. In: *Annals of Human Genetics* 7.4 (1937), pp. 355–369.

[28] P.-F. Verhulst. “Notice sur la loi que la population suit dans son accroissement”. In: *Correspondence Mathematical Physics* 10 (1838), pp. 113–126.

[29] X. Wang. “Exact and explicit solitary wave solutions for the generalised Fisher equation”. In: *Physics Letters A* 131.4-5 (1988), pp. 277–279.

[30] G. Hariharan, K. Kannan, and K. Sharma. “Haar wavelet method for solving Fisher’s equation”. In: *Applied Mathematics and Computation* 211.2 (2009), pp. 284–292.

[31] M. J. Ablowitz and A. Zeppetella. “Explicit solutions of Fisher’s equation for a special wave speed”. In: *Bulletin of Mathematical Biology* 41.6 (1979), pp. 835–840.

[32] M. J. Simpson et al. “Cell proliferation drives neural crest cell invasion of the intestine”. In: *Developmental Biology* 302.2 (2007), pp. 553–568.

[33] D. F. Newgreen et al. “Differentiation of sympathetic and enteric neurons of the fowl embryo in grafts to the chorioallantoic membrane”. In: *Cell and Tissue Research* 208.1 (1980), pp. 1–19.

[34] E. J. Crampin, E. A. Gaffney, and P. K. Maini. "Reaction and diffusion on growing domains: Scenarios for robust pattern formation". In: *Bulletin of Mathematical Biology* 61.6 (Nov. 1999), pp. 1093–1120.

[35] P. Maini and M. Solursh. "Cellular mechanisms of pattern formation in the developing limb". In: *International Review of Cytology*. Vol. 129. Elsevier, 1991, pp. 91–133.

[36] E. Crampin and P. Maini. "Modelling biological pattern formation: the role of domain growth". In: *Comments in Theoretical Biology* 6.3 (2001), pp. 229–249.

[37] J. D. Murray and M. Myerscough. "Pigmentation pattern formation on snakes". In: *Journal of Theoretical Biology* 149.3 (1991), pp. 339–360.

[38] K. Painter, P. Maini, and H. Othmer. "Stripe formation in juvenile Pomacanthus explained by a generalized Turing mechanism with chemotaxis". In: *Proceedings of the National Academy of Sciences* 96.10 (1999), pp. 5549–5554.

[39] C. J. Penington, B. D. Hughes, and K. A. Landman. "Interacting motile agents: Taking a mean-field approach beyond monomers and nearest-neighbor steps". In: *Physical Review E* 89.3 (2014).

[40] B. J. Binder and K. A. Landman. "Exclusion processes on a growing domain". In: *Journal of Theoretical Biology* 259.3 (2009), pp. 541–551.

[41] B. L. Cheeseman et al. "Cell lineage tracing in the developing enteric nervous system: superstars revealed by experiment and simulation". In: *Journal of the Royal Society Interface* 11.93 (2014).

[42] K. Kretzschmar and F. M. Watt. "Lineage tracing". In: *Cell* 148.1-2 (2012), pp. 33–45.

[43] B. J. Binder et al. "Modeling proliferative tissue growth: A general approach and an avian case study". In: *Physical Review E* 78.3 (2008).

[44] R. LeVeque. *Finite difference methods for ordinary and partial differential equations: steady-state and time-dependent problems*. Vol. 98. SIAM, 2007.

[45] C. Moler. *Numerical Computing with MATLAB: Revised Reprint*. Vol. 87. SIAM, 2008.

[46] A. N. Kolmogorov, I. Petrovsky, and N. Piscounoff. "Étude de l'équation de la diffusion avec croissance de la quantité de matière et son application à un problème biologique". In: *Bull Univ État Moscou Sér Int A* 1 (1937), pp. 1–26.

[47] K. A. Landman, M. J. Simpson, and D. F. Newgreen. "Mathematical and experimental insights into the development of the enteric nervous system and Hirschsprung's Disease". In: *Development Growth and Differentiation* 49.4 (2007), pp. 277–286.